AA FLOW DYNAMICS, MAUNA LOA 1984

By Peter W. Lipman *and* Norman G. Banks

ABSTRACT

The March 25–April 14, 1984, northeast-rift eruption of Mauna Loa Volcano, Hawaii, provided an exceptional opportunity to study development of a large basaltic aa flow system for several weeks. The major flow reached 27 km from its source vent within a few days of start of the eruption, and, fed at a rate of about 10^6 m³/h, developed an initially simple geographic zonation in aa textural types and flow morphology. Decreases in eruption rate during the first few days, to about 0.4×10^6 m³/h, triggered a channel blockage and breakout to generate a second major flow on March 29. Without further major changes in vent output from March 30 through April 7, the flow evolved from a single narrow tongue with an efficient channel, which delivered virtually the entire vent output to within 1 km of the toe, to an uprift-migrating stagnating channel system characterized by blockages, ponding, and complexly branching overflows. Lava production again began to decline after April 7, and the rate of upflow stagnation accelerated.

A major cause of the stagnation was breakdown in the hydraulic efficiency of the channel. Floating channel debris (lava boats), created by collapse of portions of the channel banks, formed dams at channel constrictions and caused ponding, overflows, and lateral breakouts that robbed the lower flow of much of its lava supply. Upflow stagnation was basically due to increasing viscosity and yield strength of the channel lava, caused by progressive degassing, formation of pasty surface clots, incorporation of channel debris, and ultimately by growth of microphenocrysts in lava stored uprift from the vent.

During the eruption, microphenocryst contents of erupted lava increased by nearly two orders of magnitude, from less than 0.5 percent to 30 percent, without concurrent change in either bulk magma composition or eruption temperature (1,140 ± 3 °C). The microphenocrysts have skeletal morphologies typical of undercooling. The increase in microphenocryst content with time was paralleled by a decrease in emission of sulfur and other gases and a decline in lava eruption rate. Growth of the microphenocrysts is interpreted as crystallization from magma that was undercooled 20–30 °C below its liquidus. The undercooling proabably resulted from separation and release of volatiles as the magma moved from the primary high-level magma reservoir at a depth of 3–5 km below the summit caldera to the 2,900-m elevation at the eruption site 12 km down the northeast rift zone. Analogous increases in microphenocryst content and accompanying uprift stagnation of lava flows have occurred during several earlier historic eruptions from Mauna Loa rift zones.

INTRODUCTION

The eruption of March 25–April 14, 1984, from the northeast rift zone of Mauna Loa Volcano, Hawaii, provided an exceptional opportunity to observe the development of a major basaltic aa flow system, fed by a high-volume eruption for several weeks. Similarly large aa flows were last erupted on Mauna Loa from the southwest rift zone in 1950 (Finch and Macdonald, 1953), before the availability of helicopters, efficient radio communications, abundant high-quality chemical data, devices for accurate temperature measurements, and other recent technological advances in monitoring techniques. In contrast, recent aa flows from nearby Kilauea Volcano (Moore and others, 1980; Ulrich and others, 1984) lasted only a few days, were fed at rates an order of magnitude smaller than the 1984 Mauna Loa activity, and generally were inaccessible to observers except in vent areas and at toes of flows (midzones are in heavily vegetated areas lacking helicopter landing points). Detailed recent observations of flow dynamics at other volcanoes, notably Etna in Sicily and Arenal in Costa Rica (Sparks and others, 1976; Wadge, 1978; Borgia and others, 1983; Cigolini and others, 1984), also involved small short-lived flows.

At Mauna Loa in 1984, we were able to observe the evolution, over a three-week period, of a complex aa flow system that achieved a maximum length of 27 km. Initial motivation for these observations was to monitor advance of the flow toward the city of Hilo (fig. 57.1*A*). As the flow terminus stagnated and hazard concerns diminished, we became increasingly intrigued by the opportunities to observe complex changes in channel efficiency related to changing parameters of lava temperature, density, gas content, petrography, and eruption rate.

Eruption rates were as high as 2.9×10^6 m³/h during the first six hours of the eruption, stabilized at 0.5×10^6–1×10^6 m³/h for the next 12 days, and slowly diminished thereafter. Total eruptive volume was approximately 220×10^6 m³. Sizeable pahoehoe flows formed only during the first day of the eruption and within a few kilometers of the vent; the remainder of the flow system consisted of aa. Especially instructive were variations in channel discharge with increasing distance from the vent during periods of steady-state lava production, variations in behavior at the flow toe as a function of slope and magma supply, development and evolution of the aa channels, and variations in density, yield strength, and viscosity of the lava as functions of time and distance from the vent. The main 1984 aa flow evolved (without major change in magma discharge at the vent) from a simple narrow tongue with an efficient channel that delivered virtually the entire lava supply to within 1 km of the toe, to an uprift-stagnating channel system with levees, blockages, ponding, and complexly branching overflows.

ACKNOWLEDGMENTS

Our channel observations would not have been feasible without the skillful assistance of helicopter pilots Bill Lacy Jr., Ken Ellard,

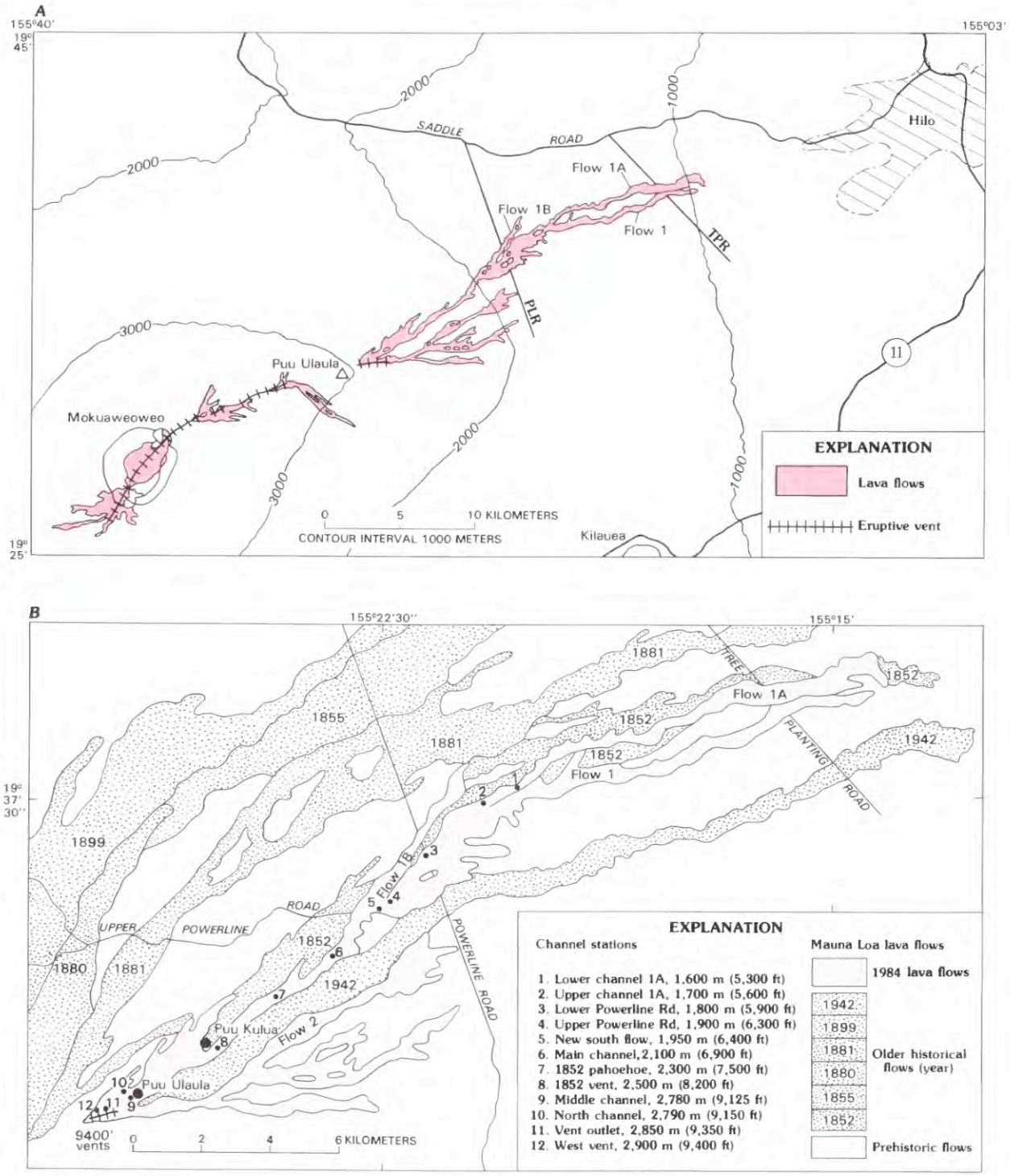

FIGURE 57.1.—Extent of lava flows from the 1984 Mauna Loa eruption. ***A***, Distribution of all 1984 flows with respect to city of Hilo (modified from Lockwood and others, 1985). All lava in the summit caldera (Mokuaweoweo) and adjacent upper parts of the northeast and southwest rift zones was erupted during the first day of the eruption (March 25). PLR, Powerline Road; TPR, Tree-planting Road. ***B***, Distribution of lava flows from the 2,900-m vent system that was active from the afternoon of March 25 until the end of the eruption on April 15. Earlier historical flows (1852, 1855, 1881, 1942) resulted from similar eruptions along the northeast rift zone. Channel stations are measurement sites for observations reported in table 57.3.

Tom Haupmann, and Ed Spencer. We also thank our many colleagues, from the USGS and academia, who assisted with the channel measurements and provided additional observations on the 1984 eruption: especially J. Buchanan-Banks, D. Clague, J. Fink, J.P. Lockwood, H.J. Moore, R.B. Moore, T. Neal, M. Rhodes, and E. Wolfe. Thoughtful reviews of earlier versions of this paper by H.J. Moore, D.A. Swanson, and G.E. Ulrich are greatly appreciated.

CHRONOLOGIC NARRATIVE

The general evolution of the 1984 Mauna Loa eruption is described elsewhere (Lockwood and others, 1985), and only the features most relevent to development of the aa flows are summarized here. The eruption began at about 0100 (all times are in Hawaii standard time) on March 25, following a nine-year repose after the 1975 summit eruption (Lockwood and others, 1976). Gradually increasing levels of seismicity and ground deformation in the previous several years had led to a forecast of increased probability of a Mauna Loa eruption in 1984–85 (Decker and others, 1983), but few precursors were evident in the days immediately preceding the 1984 outbreak.

Initial activity on March 25 broke out in the summit caldera (Mokuaweoweo) and the uppermost southwest rift zone; after about 0400, activity migrated into the upper northeast rift zone and diminished in the summit area. During that day, vents from the 3,500-m level of the northeast rift zone fed a lava flow that extended about 5 km down the southeast flank (fig. 57.1*A*). At about 1630 on March 25, new fissure vents opened at elevations of 2,800–2,900 m; they became the sites of all lava production for the remainder of the eruption (fig. 57.1*B*). By March 26, activity along the new lower fissures had become concentrated at four areas of fountaining and growth of spatter ramparts, informally designated vents 1–4, and had generated four flows that spread rapidly downslope to the east (fig. 57.2*A*) The three southerly flows (flows 2–4) stagnated by March 27, as lava production diminished from the more easterly vents (2–4), while a relatively constant volume of lava was maintained in the more northerly flow 1. Continued slow oozing of lava at the site of vent 4, accompanied by little or no fountaining, gradually built a broad lava shield 150 m high in late March and early April.

This paper considers primarily the evolution of flow 1 and its channel system, which were active from March 25 to April 13. By March 29, flow 1 had reached the 1,100-m level, 25 km from its source vent, as a relatively simple narrow flow fed by a well-developed central channel 20–50 m wide that extended to within 1–2 km of the flow front (figs. 57.2*B*, *C*, 57.3). In the early morning of March 29, a blockage and overflow at the 1,800-m level took most of the supply away from the lower reaches of flow 1 and generated a new tongue farther north (flow 1A). Flow 1 stagnated 27 km from its source at about 870-m elevation.

Flow 1A reached about 900-m elevation by April 5, when a major overflow—again at the 1,800-m level—cut off most of its supply and created a new fast-moving flow (1B) north of 1A. During April 5–8, repeated blockages and overflows prevented sustained lava supply to any organized flow below the 1,850-m level. On April 7, lava production at the vent and in the upper channel began to diminish, increasing the rate of uprift stagnation along upper parts of the flow. Lava production continued to decline, accompanied by stagnation of lower reaches of the flow system, and by April 10 no active flow toes extended below 2,450 m. By April 13, the lowest active flow toe was at 2,750 m, only about 2 km from the vent. All lava production at the vent ceased late on April 14.

Decreases in rate of lava production were paralleled by declines in volume of gas emissions. Rates of sulfur dioxide production decreased especially rapidly during the first week of the eruption (Casadevall and others, 1984). Gas emissions were intense from fissures at 3,000–3,500 m along the rift zone throughout the eruption, and as lava production began to decline at the 2,900-m vents, visible gas emission from the higher fissures began to exceed that from the active lava vents.

FLOW TYPES

Both aa and pahoehoe flow types encompass much variation in lava textures (Wentworth and Macdonald, 1953; Macdonald 1972) that can provide information on the kinematics of flow and on lava rheology (Swanson, 1973; Peterson and Tilling, 1980). During the 1984 Mauna Loa eruption, distinctive aa flow types tended to develop as functions of distance from the vent, steepness of terrain, and mechanism of the flow advance. Some of these lava types have not previously been described or interpreted in terms of emplacement kinematics. Lava from the 1984 Mauna Loa eruption includes most of the pahoehoe types recognized on Kilauea (Swanson, 1973), transitional lava between pahoehoe and aa, and diverse aa types—slabby, clotted, spiney, scoriaceous, clinkery, and blocky. These flow types could also be identified within lava channels on the basis of textures developing on the surface crust. General relations among the flow types in the 1984 eruption are summarized here; detailed features of a few are discussed in later sections, where their origin is closely tied to evolution of other flow features such as flow toes, channels, and levees.

PAHOEHOE

Typical fountain-fed shelly pahoehoe formed in the vent area, at 2,850–2,900-m elevation early during the eruption, but extended as pahoehoe for only about 2 km, to about the level of Puu 9,146 (2,790 m) before changing to aa—probably within less than two hours after the source vents opened. As soon as a channel was well established to this level, virtually all lower lava fronts advanced as aa. The limited extent of pahoehoe may reflect the steeper slopes of this sector of the rift zone (4°–6°), the viscous character of the 1984 lava, or some additional process. Where able to flow slowly (less than 10–15 km/h), lava in the developed channel of flow 1 was capable of generating pahoehoe down to at least the 2,400-m level, about 5 km from the vent, as shown by small pahoehoe overflows during the first hours of the eruption. After March 26, however, the channel delivered lava so efficiently to lower reaches of the flow that no lava front advanced as pahoehoe until the last days of the

A

FIGURE 57.2.—Active flow front and channels, 1984 Mauna Loa eruption. ***A***, Rapidly advancing toe of flow 1 at 2030 H.s.t. on March 25, about 2 hours after initiation of lower vents. Toe is at about 2,400-m elevation, advancing at estimated 2 m/s. Photograph by R.B. Moore. ***B***, View uprift toward 2,900-m vents on March 27. Flow 1 channel is on right; smaller channels feed flows 2 and 3 on left. ***C***, Flow 1 toe at 1,350-m elevation, looking downrift on March 27. Channel is well developed and about 50 m wide; it extends to within 1 km of flow toe, marked by smoke from burning forest.

eruption, when blockages and disruption of the channel again permitted pahoehoe overflows from the channel within 1–2 km of the vents.

TRANSITIONAL LAVA

Because the transition from pahoehoe to aa occurred within the confined channel of flow 1 during much of the eruption, we had ample opportunities to observe this change from a helicopter and from observation stations along channel levees. Our observations on the 1984 lava are in accord with the interpretations of Macdonald (1953) and Peterson and Tilling (1980) that the transition from pahoehoe to aa involves the relation between viscosity and rate of internal disturbance due to flowage (shear strain). If flow mechanics (flow volume, flow dimensions, slope, momentum) impel pahoehoe to continue to move and deform after it has become highly viscous, the lava will change to aa if the critical relation has already been approached. Approach to this critical condition can be recognized when the flow surface is littered with solid and semisolid blebs and blocks that disrupt flow streamlines in the channel.

AA TYPES

Different aa lava types reflect interrelated aspects of magma rheology, gas content, terrain effects, and flow rates. Lava viscosity and yield strength generally increase downstream because of decreased gas content, decreased average bulk temperature of the flow, increased crystallization of microphenocrysts, and incorporation or formation of solids, as discussed later (also see Moore, chapter 58). The net effect is to trigger successive irreversible changes in aa texture, similar to those accompanying the pahoehoe-aa transition.

B *C*

FIGURE 57.2—Continued.

SLABBY AA

In the 1984 Mauna Loa eruption, aa flows nearest the transition from pahoehoe tended to form slabby aa (also called slabby pahoehoe), which consists simply of pahoehoe crust completely disrupted in slabs by flowage at a rate too great for the crust to accommodate the shear strain plastically (fig. 57.4*A*). Slabby aa was well developed in the advancing terminus of flow 1 at elevations of 2,450–2,600 m, about 3–5 km from the vent.

SCORIACEOUS AA

Farther downflow, where the lava was slightly denser and more viscous, the surface of the channel no longer maintained a smooth pahoehoe surface crust. Instead, it developed scattered lumps or clots of relatively cool scoriaceous lava, separated by more fluid incandescent lava retaining crude pahoehoe character (fig. 57.4*B*). When overflows or breakouts of such scoriaceous aa occurred fairly slowly, and flow fronts advanced no faster than 1–2 m/min, this lava type retained its clotted texture as it cooled. The frothy clots consisted of red-brown oxidized scoria masses 5–30 cm across, set in dark gray smoother less vesicular lava having a thin poorly developed glassy surface. When overflow rates were more rapid, as in a sudden sheet-flow breakout through a breached levee, the entire surface of the resulting flow disaggregated into scoriaceous lumps, and the surface of the resulting deposit consists of loose oxidized scoria lumps totally covering the dense interior of the aa flow. This lava type has at times been called spiney aa (Macdonald and Abbott, 1970, p. 26) because of the jagged irregular surfaces of the scoria lumps. The front of flow 1 during its advance on March 25–26 was dominantly scoriaceous aa between elevations of about 2,450 and 1,850 m, at distances of 5–12 km from the vent.

CLINKERY AA

Even farther downflow, the active lava surface in the channel consisted largely of cooled clots of relatively dense lava that ground against each other while riding on top of the more fluid lava core in

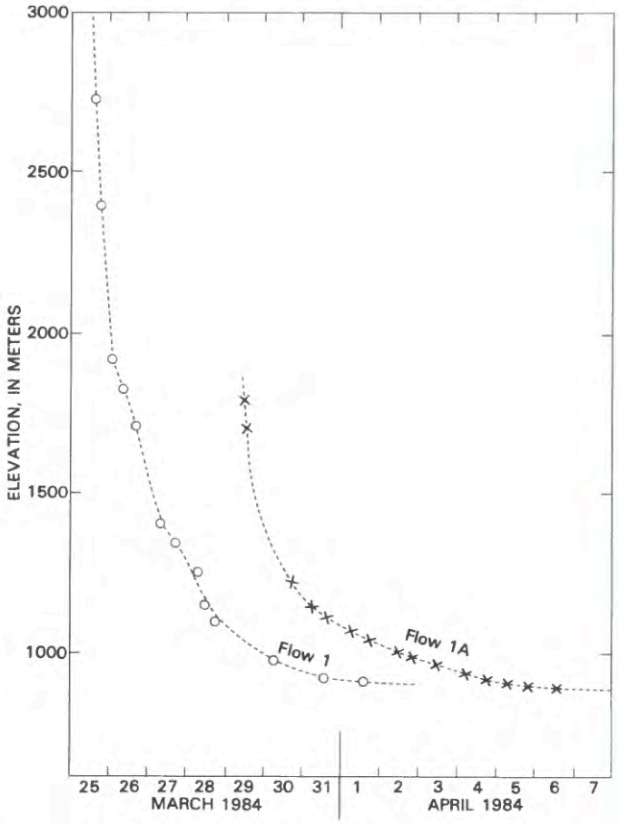

FIGURE 57.3.—Change in elevation of lava-flow toes during 1984 Mauna Loa eruption.

A

B

C

FIGURE 57.4.—Aa lava types observed on April 3, 1984. ***A***, Slabby aa at 2,500-m elevation, overlying spatter from the 1852 vent. Active channel is visible at upper left (arrow). Radio at lower right is 20 cm long (excluding antenna). ***B***, Scoriaceous aa flow top at 1,800-m elevation. Scoria blocks are uniformly small in size, averaging about 10 cm in diameter. Smoother crust between clusters of scoriaceous aa marks points of late stretching of the flow surface and upwelling of degassed lava. ***C***, Blocky aa, at 1,600-m elevation. Tripod and figures at right are on stable marginal levee. Center of flow, at left edge of photograph, contains a broad weakly developed aa channel. Site is near the downflow gradation from the transitional to the dispersed flowage zone (see fig. 57.5).

the channel. Breakouts and overflows of this material formed dark gray clinkery aa, which contrasts with the scoriaceous aa in having angular rather than scoriaceous surfaces, and in being darker in color, less oxidized, and less vesicular. During early advance of flow 1 and the later flow 1A, the gradual transition from scoriaceous to clinkerly aa occurred at elevations of 1,850–1,700 m, about 12–15 km from the vent.

BLOCKY AA

Along the lower reaches of flow 1, below about 1,500-m elevation and more than about 20 km from the vent, the lava largely solidified beneath a rubble cover of dense dark gray blocky aa (fig. 57.4C). Blocky aa is similar to the so-called block lava characteristic of many andesitic flows (Macdonald, 1972), although surfaces of the aa blocks are less smooth because of vesiculation. Some resulting blocks are as large as several meters across. This material was rafted farther downflow on viscous but still fluid underlying material, mixed with more scoriaceous clinkers and lumps carried from higher in the channel, and finally deposited along the toe or margins of the flow as heterogeneous rubble.

AA FLOWAGE ZONES

Early development of the 1984 aa flows (especially flow 1 during March 26–29) displayed systematic variations in structure and morphology from vent to toe—in addition to the aa textural types just summarized—that can be described in terms of four zones: flow toe, lower dispersed flowage, transitional channel, and upper stabilized channel (fig. 57.5). Subsequent development of blockages, ponds, and overflows of lava complexly overprinted this simple initial aa flow zonation, but each of the relatively ephemeral blockage-overflow lobes tended to show a similar zonation.

FLOW TOE

Early in the eruption, most features of the aa flow system were established within a few kilometers of the flow toe during its advance. Upper well-channelized parts of the flow were stable and changed little, as virtually all lava moved efficiently down the channel to the toe area. The character of the flow toe varied mainly as a function of slope of the local land surface and distance of the toe from the stabilized channel.

Near the vent, on steeper slopes, and where the channel was well established close to a flow toe, fluid lava was delivered efficiently to the flow toe. The result was a rapidly moving broad flow front, consisting of scoriaceous or slabby aa, only 1–3 m high and with a nearly flat upper surface (figs. 57.2*A*, 57.6*A*). Such rapidly moving fronts exposed the liquid core of the aa flow as a bright orange band along the entire flow front; the flow advanced by outwelling of the fluid core, which then crusted over, brecciated, and overrode its front. This process produced a poorly developed basal breccia, because the brecciated upper surface moved more slowly than the center of the flow advanced. Such flow fronts tended to form scoriaceous or clinkery aa. Observed velocities at these flow fronts varied from 50 m/h to as much as 5 km/h. This type of flow front was observed during early stages of breakouts from the main channel where relatively fluid ponded lava was released as sheet flows, even late in the eruption (fig. 57.6*A*). Similar features probably were dominant during the early rapid advance of flow 1 on March 25–26.

In contrast, on gentler slopes, at sites more distant from the vent, and where a broader zone of dispersed flow occurred below the channelized flow, the flow toe moved more slowly, was higher and more irregular in profile, and consisted of denser blockier lava (fig. 57.6*B*). Little or no fluid material was visible at the flow front, and the steep high front advanced by spalling of dense blocks and slabs, largely from the breccia layer riding on top of the advancing flow. Fine granular to dusty material, resulting from abrasion of aa blocks, was a significant constituent at the flow toe. Velocities at this type of flow front varied from a maximum of 50 m/h to stagnation. Such flow characterized the fronts of flow 1 and flow 1A during their slow advance below about 1,350 m elevation.

ZONE OF DISPERSED FLOW

Behind the advancing toe of the 1984 lava was a zone in which movement was dispersed across much of the flow width and a central channel was poorly developed or absent. During rapid advance of flow 1 early in the eruption, the zone of dispersed flow was relatively short; on March 27 this zone extended only about 1 km up from the toe at the 1,350-m level (figs. 57.2*B*, 57.7). As the eruption progressed, the flow toe became more sluggish, and the zone of dispersed flowage extended as much as 5–10 km up the flow. Observations in this zone were sparse, because the lava was still hot and unstable, and surface features were difficult to observe from terrain adjacent to the flow. Movement at the upper surface of the flow tended to occur along discrete shears, between which ridges of blocky aa moved fairly coherently. Near the toe, the most rapidly moving central part of the flow consisted of blocky aa showing little or no incandescence; farther upstream, the center of the flow was more incandescent and graded into a defined central channel containing visible fluid lava. Flow velocities increased gradually from

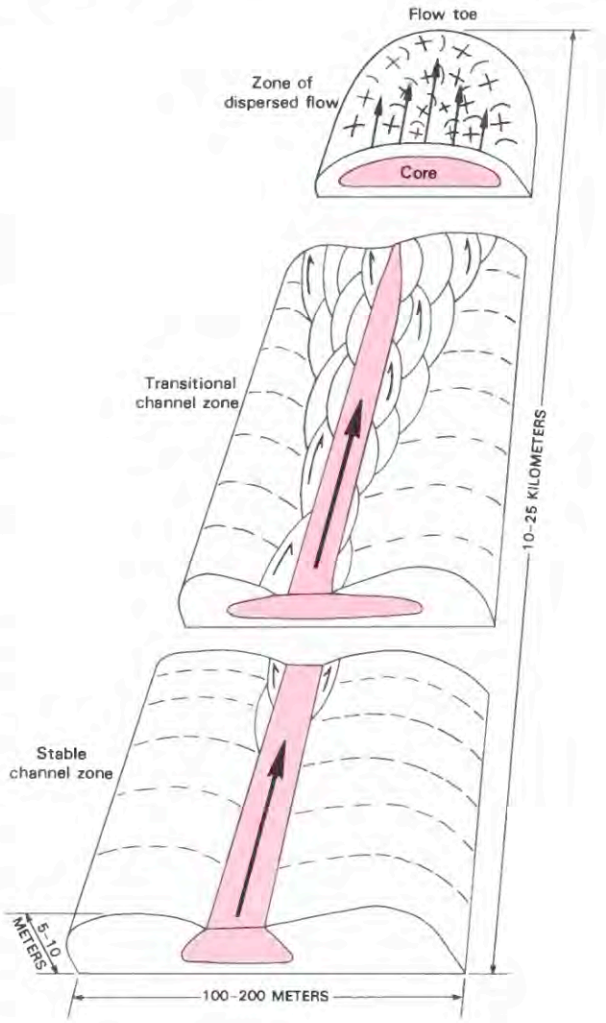

FIGURE 57.5.—Diagram showing contrasting structural features of aa channel zones.

A

B

FIGURE 57.6.—Aa flow fronts. ***A***, Fast-moving front of flow 1B, characterized by low toe (1–3 m) and exposed fluid core. Note lava boat (arrow) being rafted toward flow front. April 5, at 1,800-m elevation. ***B***, Slow moving front of flow 1A, characterized by higher toe (10–15 m) and rubbly incandescent front. A minimum temperature measured at flow front (not in fluid core) at this site was 1,086 °C (table 57.1). March 31, at 1,150-m elevation.

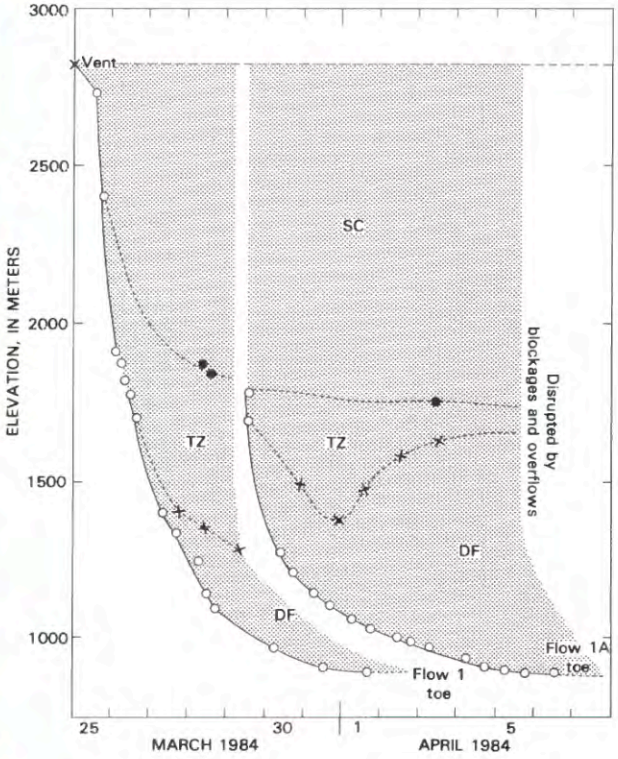

FIGURE 57.7.—Distribution of channel zones in relation to time and elevation, 1984 Mauna Loa lava flows. SC, stable-channel zone; TZ, transition zone; DF, zone of distributed flow. Circle, position of flow toe; x, DF-TZ transition; dots, TZ-SC transition.

the margin to the interior of the flow. Axial velocities were as much as several kilometers per hour; more typically, they were a few hundred meters per hour. Cross-sectional profiles through this zone of the flow are typically convex upward for slow-moving flows but nearly flat for rapidly advancing flows. At times, when a fast-moving flow crossed a steep slope, the channelized center of the flow could break through the more dispersed and sluggish lower part of the flow, delivering fluid lava to a flow front that had previously been more sluggish.

TRANSITIONAL CHANNEL ZONE

The transition between zones of dispersed flowage and the stabilized channel was marked by the presence of a distinct channel containing incandescent clinkery aa, bounded by blocky or clinkery lava a few tens of meters wide that was still capable of deforming and moving slowly (figs. 57.5, 57.8*A*). These marginal areas consisted of multiple ridges or lenses of blocky lava, bounded by discrete shears (fig. 57.8*B*); they continued downstream into similar features in the zone of dispersed flow. The active channel in the transition zone was generally wider than in the stable channel zone. Toward the zone of dispersed flow, the active channel again decreased in

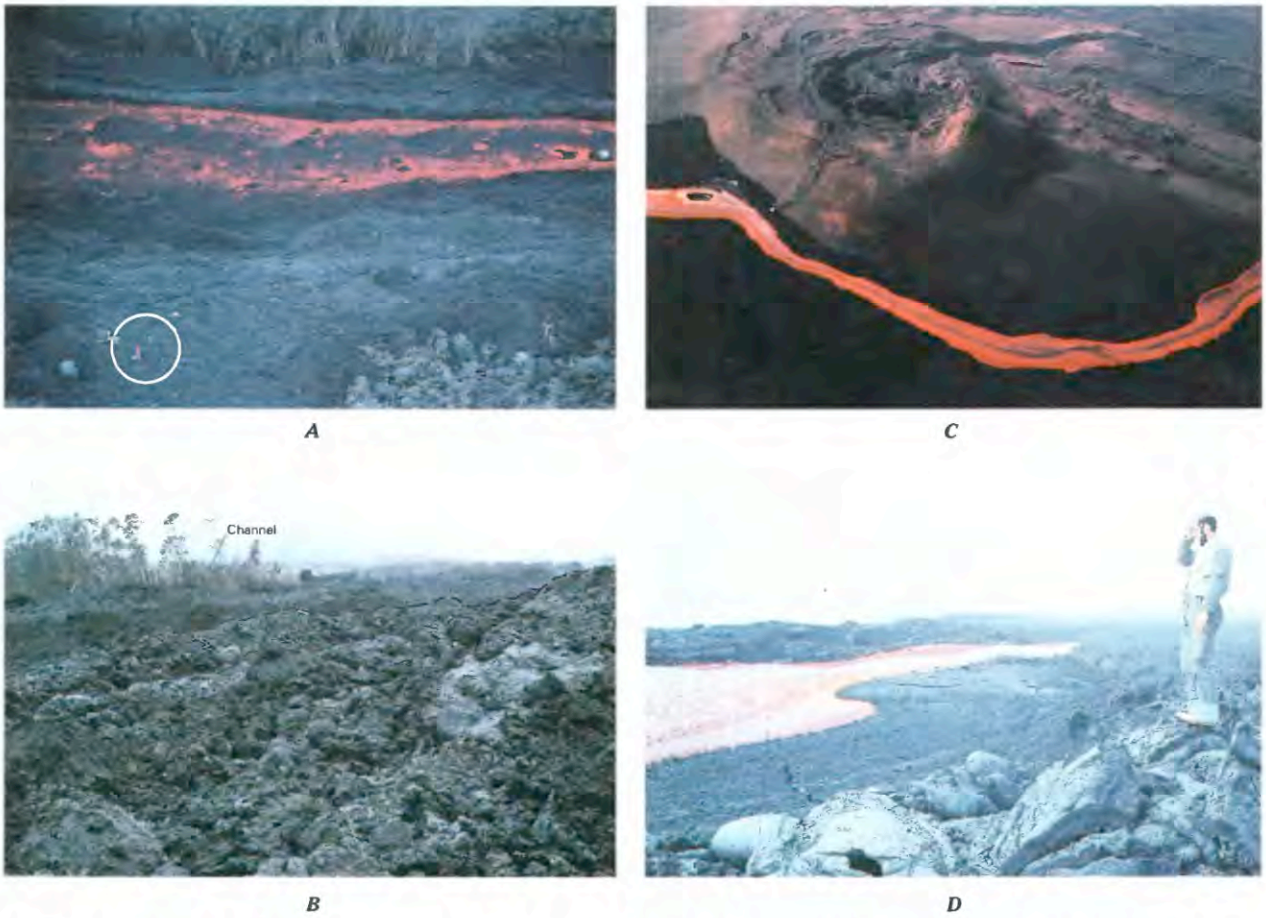

FIGURE 57.8.—Features of stable-channel and transition zones, 1984 Mauna Loa flows. ***A***, Aerial view of channel in transition zone at channel station 1, 1,600-m elevation. Active incandescent channel, about 24 m wide and flowing at 3.4 km/h (table 57.3, no. 1), is flanked by marginal shears in blocky aa moving at only a few meters per minute. Lava balls and other solidified debris are abundant on channel surface. Persons (circled) are standing on stable marginal levee. Photograph taken March 31. ***B***, Shear lenses adjacent to channel margin in transition zone at station 1, 1,600 m. Near ridge at right is stable early formed marginal levee; three shear lenses are present (boundaries marked by dashed lines), and weakly developed aa channel is visible at upper left. Photograph taken April 2. ***C***, Aerial view of stable channel zone at 2,500 m. Channel has been well established since first day of eruption. Dark band in center channel marks maximum velocity zone (19–20 km/h; table 57.3, no. 43–44). Vent of 1852 eruption is in upper part of photograph; channel station 8 is at far right. Photograph by J.D. Griggs, March 30. ***D***, Stable channel zone at station 8, 2,500 m. Man stands on original overflow levee; margin of channel has crusted over, although lava continues to flow beneath thin crust. Photograph taken April 2.

width as the number of marginal shear lenses increased. Individual shear ridges or lenses were several meters wide and traceable longitudinally for tens of meters. Measured flow velocities in the central channel of this zone were as much as 25–50 m/min (2–3 km/h); typical velocities in the marginal shear lenses were 1–3 m/min, with maxiumum velocities accompanying passage of lava surges in the central channel.

In addition to longitudinal movement, the belts of shear ridges inflated and subsided as much as several meters vertically in response to changes in lava levels in the channel. The combined vertical and longitudinal motions indicate that the belts of shear ridges were underlain by fluid lava hydraulically connected to the active channel. In comparison with the zone of dispersed flowage, the fluid core of the flow in the transitional-channel zone was more restricted but still covered a broader area than that of the channel. Audible creaking noises, reflecting hydraulic adjustments of the crust over marginal portions of the core, accompanied passage of lava surges in the adjacent channel. The presence of a sluggish fluid core beyond the margins of the channel 9 days after channel stablilization was documented during leveling toward the channel on April 4, at the 1,900-m monitoring station: 29 m from the active channel, the elevation decreased 10 cm as the lava level in the channel dropped in response to passage of a surge.

Early in the eruption, when flow 1 and then flow 1A were advancing rapidly, the transition zone was broad. On March 28, it extended from within 1–2 km of the flow 1 toe (then at the 1,200-m level) to above the 1,850-m level (fig. 57.7), about 10 km up the flow. Later, as advance of flow 1 and then flow 1A slowed, the zone

of dispersed flow extended 5–10 km up from the toe of flow 1A, but the zone of stablized channel flow began to encroach downslope on the transition zone. By April 3, the transition zone on flow 1A had decreased to a length of 3–4 km, from about 1,750 to 1,600-m elevation.

STABILIZED CHANNEL ZONE

As the lava lens adjacent to the active channel cooled and marginal deformation of the flow ceased, all movement became concentrated in the central channel, producing a stable geometry in upper reaches of the flow (fig. 57.8*C*, *D*). Above about 2,450 m, where flow 1 had advanced rapidly as a sheet only a few meters thick during March 25–26, the channel appears to have stabilized rapidly, and there is little evidence for ephemeral development of a transition zone. In contrast, the segment from about 2,450–1,850 m elevation, although part of the stable channel zone by March 28, contains structures (broad central depression, inward-facing sags and ridges, and open cracks parallel to the channel) that indicate that this segment passed through a transition zone earlier during the eruption. By March 28–29, just before the breakout of flow 1A, the lower margin of the stable-channel zone was at about 1,850–1,900 m, below channel observation station 4 at 1,900 m and above station 3 along the Powerline Road at 1,800 m (fig. 57.1*B*). By April 3, the flow 1A channel had stabilized at the breakout area at about 1,800 m, but it never stabilized below about 1,750 m. After flow 1B and related breakouts at the 2,100-m level on April 5 had pirated the lava supply from lower parts of the previously stable channel zone, successively higher segments of the channel were abandoned or covered by lava from breakouts higher along the distributary system.

CHANNEL EVOLUTION

A notable feature of the 1984 eruption was evolution of the main flows and associated channels from a simple long and narrow flow to a more complex geometry, largely as a result of breakdown in the efficiency of the lava channel. A key feature in this evolution was the formation of lava boats by rafting away of unstable portions of the lava channel. The lava boats caused blockages and ponding at downstream constrictions in the lava channel.

INITIAL CHANNEL DEVELOPMENT

Lava channels formed in all 1984 Mauna Loa aa lobes more than a few hundred meters long, in response to the transverse velocity gradient across the flow near its toe, and by upflow stabilization of the flanks of the flow (figs. 57.5, 57.9). The position of the lowest well-defined channel coincided approximately with the diffuse boundary between the transition zone and the zone of dispersed flow. The first indication of this boundary was an upflow change in the cross-sectional flow profile, from convex upward near the toe (fig. 57.9*A*, *B*), to a broad rounded M-shaped profile upflow (fig. 57.9*C*). This change resulted from draining of lava toward the flow toe, with the greatest velocity in the central trough. Higher in the transition zone, the flow velocity of the axial zone increased further (fig. 57.10), and the velocity gradient between the rapidly moving central area and the stagnating margins became greater and eventually abrupt. This change confined a progressively greater volume of faster moving lava to a smaller channel cross section in an upstream direction. The surface of the central area became more incandescent and finally consisted dominantly of fluid lava (fig. 57.9*C*, *D*)

The geometry of the channel appeared to be sensitively related to other parts of the flow, especially in its lower reaches where the channel remained in dynamic interaction with the associated lava lens that extended as much as tens of meters beneath more stable flanks of the flow. The upper 10 km of the 1984 aa channel—above about 1,850-m elevation—remained stable for 8–10 days after its formation (fig. 57.7), but the lower reaches that never became part of the stable channel zone were sensitive to subtle changes in eruptive volume and lava properties. These changes produced floating debris in the lava channel that eventually caused blockages, ponding, and overflows of lava. This depleted the lava supply to lower channel reaches, and both the blockages and flow progressively stagnated upslope.

LAVA BOATS

Floating debris of solidified lava was conspicuous in lower reaches of the channel as early as March 27, when channel observations were first undertaken more than a few kilometers from the vent. Large rounded lava masses found on consolidated surfaces

FIGURE 57.9.—Development of the aa channel and levees during the 1984 Mauna Loa eruption. ***A***, Initial aa sheet flow; near toe in zone of dispersed flow. ***B***, Mature aa sheet flow. Zone of dispersed flow; flow has spread laterally and inflated as supply of lava increases. ***C***, Transition zone, showing incipient development of a channel and the rounded M-shaped profile. Solid line indicates flow level at early stage of high lava supply; dashed line indicates lower flow level at later stage, when lava is draining efficiently downflow to zone of dispersed flow and central channel is becoming established. A peripheral zone of sluggish flow has developed along the margins and bottom through degassing, drag, and cooling. The flow has spread and the early levees have grown by overflows and lateral bulldozing during periods of high lava supply. Marginal shear ridges are active above the areas of sluggish flow. ***D***, Development of stable channel. Zone of sluggish flow has developed a more stable solidified crust, beneath which a plastic lava core remains, and erosion may have deepened the axial zone of sluggish flow, thereby deepening the channel and permitting higher flow rates. Also shown are overflow levees adjacent to the narrower deeper channel. ***E***, Mature channel in zone of stable flow. Lateral restriction of channel through inward migration of the zones of solidification and sluggish flow is counterbalanced by continued growth of overflow levees and perhaps by further erosion at the bottom of the channel. ***F***, Alternative types of levees for stage shown in *D*, showing development of structural levees. 1: Similar to *D*, but without development of overflow levee. 2: Uplift and buckling of the early channel crust during period of high lava supply. ***G***, Alternative types of levees for stage shown in *E*, showing concurrent development of overflow and deformation levees. 1: Overflow levee growing adjacent to earlier deformation levee, over regenerated channel crust. 2: Both levees bulldozed laterally during periods of high lava supply, overturning the earlier deformation levee (see fig. 57.16*B*).

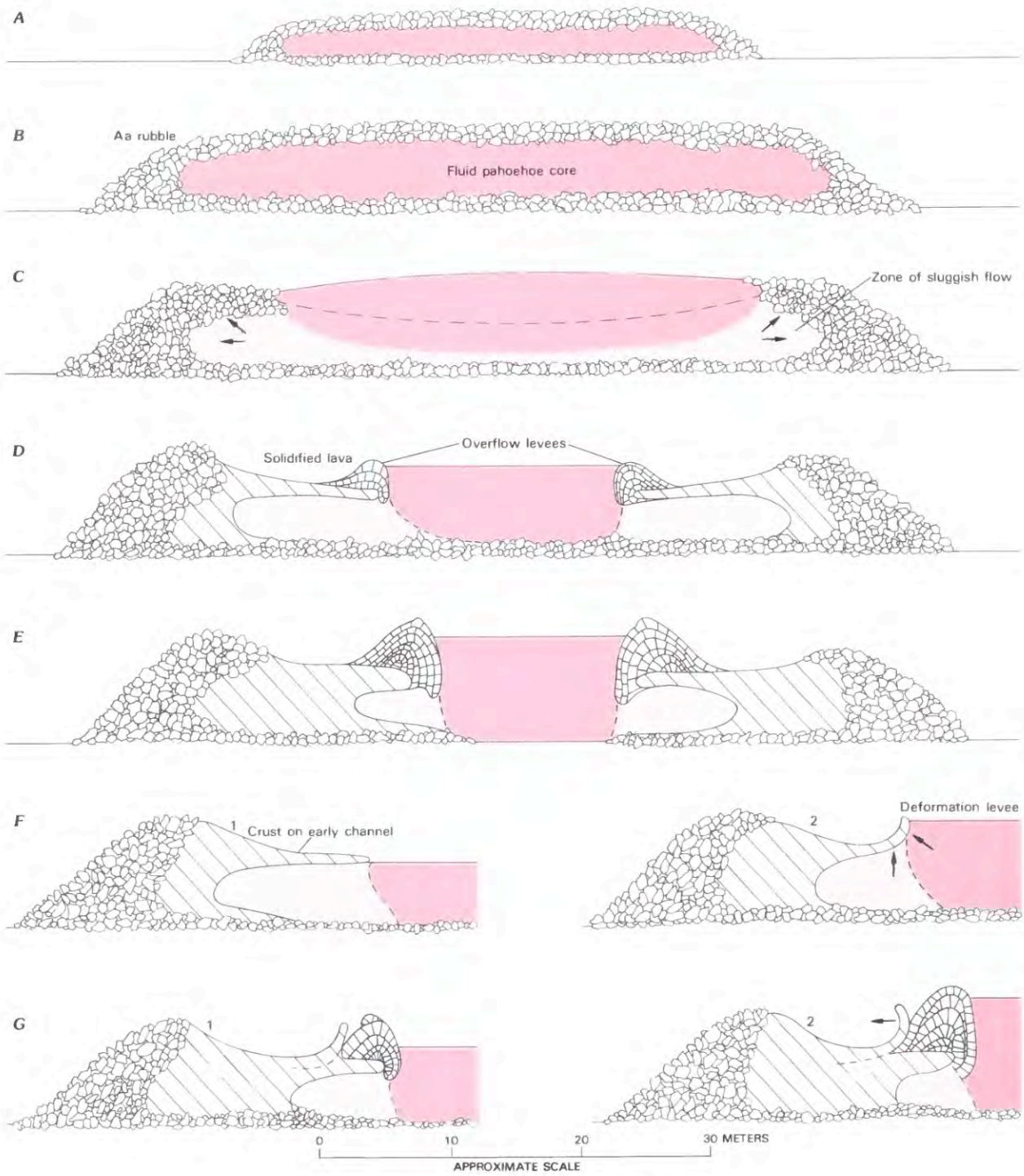
A
B
Aa rubble
Fluid pahoehoe core
C
Zone of sluggish flow
D
Solidified lava
Overflow levees
E
F
1
Crust on early channel
2
Deformation levee
G
1
2
0
10
20
30 METERS
APPROXIMATE SCALE

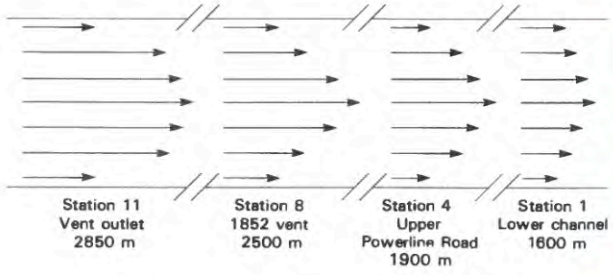

FIGURE 57.10.—Diagrammatic representation (plan view) of across-flow variation in flow velocity, channel of flow 1–1A. Station locations shown on figure 57.1*B*.

of aa flows have been called accretionary lava balls and interpreted as having formed "by the rolling up of viscous lava around some fragment of solidified lava as a center, in much the same way as a snowball rolling downhill" (Wentworth and Macdonald, 1953, p. 64). During the 1984 eruption, we referred to such features as lava boats, to emphasize their origin by caving and rafting within the active lava channel (fig. 57.11*A*), rather than by rolling on the clinkery surface in lower reaches of the flow.

Lava boats and more irregular small debris were observed to form by caving of unstable overhanging channel banks and walls, especially when the level of lava in the channel dropped and so reduced support for the bank (fig. 57.11*B*). Caving and rafting of the channel banks was aided by the presence of still-plastic lava under the channel margins (fig. 57.9), particularly adjacent to marginal shears in the transition zone. In the zone of stabilized flow, some overhangs also originated as partial roofs of incipient lava tubes. Major collapse events along the channel banks were marked by dust clouds and by subsequent increase in the number of lava boats downstream.

Lava boats also formed along the inside banks of meanders, where flowing lava in the channel applied drag and compression and opened tension cracks in the adjacent bank (fig. 57.12) Continued pressure by the moving lava then rafted fragments of the bank into the channel to form lava boats. Such formation of the lava boats tended to straighten the channel with time, in contrast to processes in rivers of water, which erode on the outsides of meanders and deposit sediment on the insides. The first channels in the early aa (fig. 57.9C) had meanders because the flow followed irregularities in the pre-eruption topography behind the toe. In addition, the flow advanced as a thin sheet in which the ratio of friction to mass was high (fig. 57.9*A*); the toe of the flow tended to inflate (fig. 57.9*B*), because the upflow channel delivered lava faster than it could be distributed by flow advance or spreading. As a result, the incipient channels initially developed a somewhat disorganized geometry as flow directions and velocities changed in response to changing rates and locations of advance of the toe. Later, as the channel deepened and narrowed (fig. 57.9*C*, *D*), the flow rate increased, and some

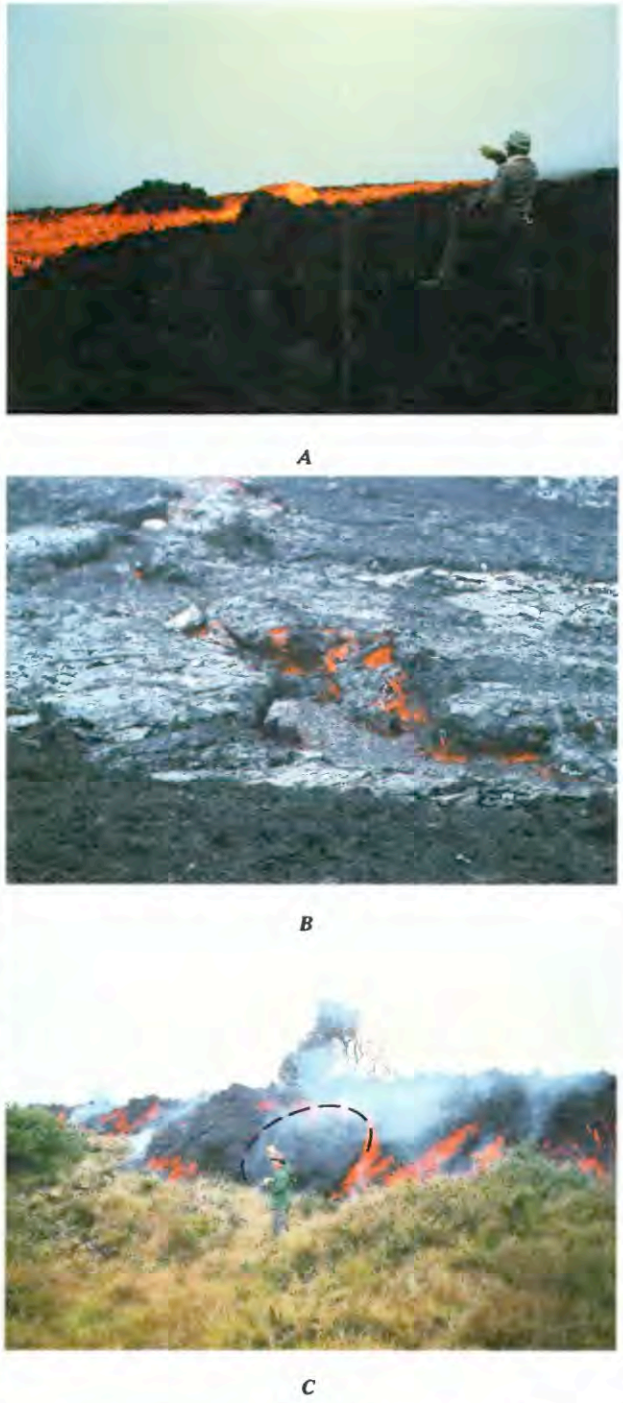

A

B

C

FIGURE 57.11.—Lava boats. ***A***, Lava boat floating in full channel during small surge. Channel is confined behind small overflow levee of scoriaceous aa. Photograph taken March 29, at 1,900-m elevation (compare with figure 57.16*B*, taken 7 days later at same site). ***B***, Formation of lava boats by collapse of overhanging levee wall into channel during low stand of lava; small satellitic northern channel. Photograph taken April 9, at 2,800-m elevation. ***C***, Flow front, showing 2-m-diameter lava boat (outlined with dashed line) being pushed ahead by advancing flow. Photograph taken April 6, at 1,700-m elevation.

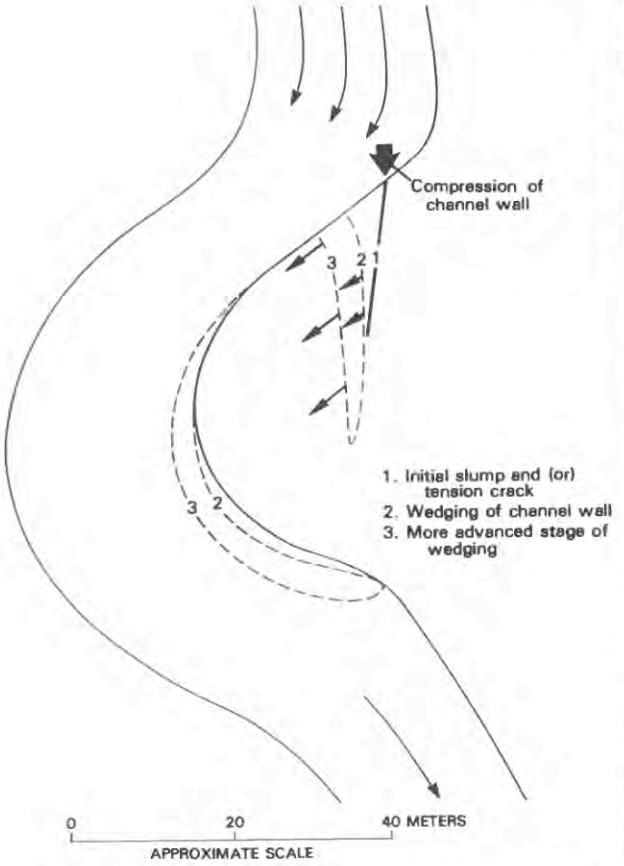

FIGURE 57.12.—Diagrammatic sketch (map view) of origin of lava boats by wedging and slumping from inside bank of channel meander in the stable-channel zone.

early meanders became inefficient for delivery of the lava to the flow front. Such channels tended to straighten through spalling of the inside walls of curves.

The elongate wedges of channel-bank and levee material thus formed floated downstream as lava boats that gradually broke into more equant shapes. Frequently, they disintegrated into equant pieces when they grounded on the channel floor or jammed against the downstream channel walls and adjacent boats. As the boats rolled and bobbed in the channel, they also accreted a lava sheath.

In the zone of dispersed flow below the active channel, the lava boats were rafted along the upper surface of the flow, in conveyer-belt fashion toward the flow front. In this zone, blocks on the flow surface tended to be carried passively downslope, with little differential movement. Thus no additional lava was accreted to the lava boats below the active channel. Frequently, lava boats several meters in diameter were rafted all the way to the flow front and pushed ahead by the advancing flow (fig. 57.11C).

Lava boats were rare in upper reaches of the channel, within about 5 km of the vent, especially during the first half of the eruption, reflecting the more stable channel configuration in this area. In the channel within 200–300 m of the vent, rapidly flowing lava splashing against the channel banks at a curve occasionally stoped large blocks from the bank. Lava boats became progressively more abundant downflow and also with increasing age of the channel.

The lava boats were useful indicators of channel velocities and minimum depths (table 57.2; app. 57.2); they also played a key role in channel evolution by causing blockages and dams in the channel. The largest lava boats were 6–7 m across and extended 2–3 m above the channel surface. Several kinds of observations suggest that they typically projected at least this distance below the channel surface, providing a minimum estimate of channel depth: (1) Most lava boats rafted to the lava surface low on the flow are subequant in shape. (2) Rarely, large lava boats would hang up on the channel floor and roll over, exposing their full geometry. Even during low channel levels, 2–3 m below maximum, large lava boats would commonly float freely—suggesting typical channel depths of 4–6 m. (3) Because the density of lava in the channel is low—about 0.5 g/cm^3 at the vent to 1.5–2.5 g/cm^3 in lower reaches (discussed later; also see fig. 57.20)—typical channel-bank debris (density 1.0–2.0 g/cm^3) is only slightly less dense than the channel lava, and the resulting lava boat could not rise buoyantly more than about one-half its diameter. As the channel lava degassed, cooled, and became more dense downchannel, accompanying lava boats probably gradually emerged higher. Lava boats that originated by caving of unstable banks from lower channel reaches (transition zone) would also be denser than boats derived from higher stretches of the channel. Within a few kilometers of the vent, most lava of the channel walls was more dense than the fluffy lava in the channel; caved fragments of channel banks probably sank rather than floated, and formed saltating blocks along the channel bottom. Only rare rafted fragments from the low-density agglutinated spatter ramparts could float in the channel lava close to the vent.

BLOCKAGES AND PONDING

Accumulation of lava boats and debris from surface crusts in channel constrictions (fig. 57.13A) caused blockages and ponding of the main channel and produced major changes in the character of the aa flow during early April. Small ephemeral blockages formed at a few channel constrictions in middle and lower reaches of the flow as early as March 27, but the first significant lava dams were not observed in well-developed reaches of the main channel until March 29. During the following week, blockages increased in size and number, and they gradually formed higher along the main channel (fig. 57.14). Overflows from long-lived ponds occurred both to the sides and over the tops of blockages (fig 57.13*B*). When overflow was sustained at one side of a dam that held, a branch flow could be generated. Most branch breakouts advanced at first as sheet flows; if the overflow was maintained, erosion of the flanking levee permitted the flow rate in the branch to increase, a channel to develop, and a stabilized branch flow to form.

By the morning of March 29, a major blockage at the 1,800-m level was able to divert the entire lava supply of flow 1 northward

A *B*

FIGURE 57.13.—Blockages and surges in lava channels, 1984 Mauna Loa eruption. ***A***, Aerial view of developing blockage along constricted sector of flow channel. Upchannel pond has relatively cool scoriaceous surface; hotter interior lava is draining downchannel from below blockage. Light-colored lava along right margin is 1852 pahoehoe. About 1,800-m level, March 31. ***B***, Aerial view of surge overflow at blockage site, looking upchannel. About 1,650-m elevation, March 31.

to form flow 1A. Many smaller blockages in the next few days caused overflows at this same general elevation. By April 4, blockages were occurring as high as 1,950 m, and on April 5 a large blockage at about 2,050 ft caused a major surge and overflow to form flow 1B. On April 6–7, repeated blockages and overflows at the 2,000–2,100-m level prevented sustained feeding of any flow system below 1,850 m. By April 8, blockages were causing many overflows at elevations as high as 2,300 m), and blockages and overflows extended back almost to the vent during the next two days.

Most debris blockages reduced, but did not stop, downchannel flow; typically, little glowing lava was visible at the surface in the constricted sector of the channel, but fluid lava would continue to flow or at least ooze out at the lower end of the constriction. The amount of lava ponded by a blockage could be large relative to the upslope channel volume; blockages and ponding promoted construction of overflow levees that in turn could be enlarged by spreading of the levees and overflow of the entrapped ponded lava. The largest ponds, at the 1,800-m and 2,050-m levels, were as much as 100 m wide, 10 m deep, and 500 m long; periodic abrupt release of much of the ponded lava could significantly modify the downstream flow regime.

A dynamic relation was established early between blockages and formation of lava boats: generation of a cluster of lava boats by failure of the channel bank provided material to cause a blockage at a downstream constriction, and in turn formation of such a blockage would lower the channel level farther downstream, causing additional failure of the channel bank and generation of more lava boats. As a corollary, when the channel level was low and few lava boats or other debris were evident in the channel, blockages and ponding could be inferred to be occurring upchannel. Both straightening of meanders and small fluctuations in channel level, perhaps initially related to short-term variations in rate of lava production at the vent, were thus capable of generating blockages farther downchannel. The intensity of such perturbations increased during the first two weeks of the eruption, even though the rate of lava production at the vent remained roughly constant, at least from March 30 to April 7.

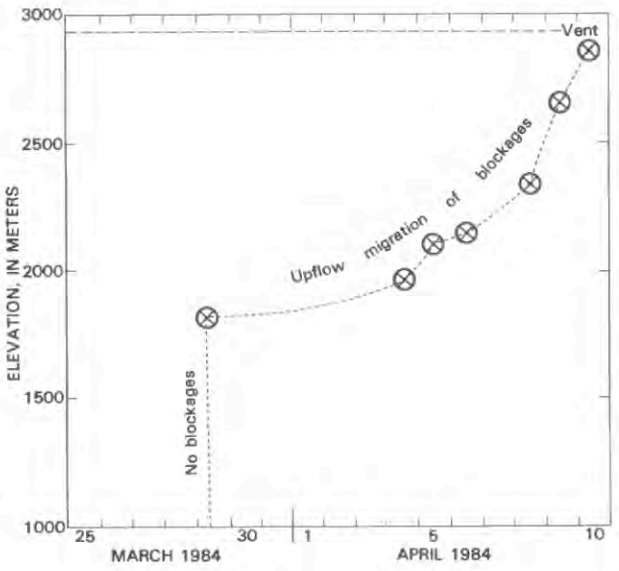

FIGURE 57.14.—Elevations of highest overflow-producing blockages (circled crosses) in main flow channel of 1984 Mauna Loa eruption.

SURGES AND OVERFLOWS

Lava that ponded behind channel blockages eventually escaped, either by overflowing the channel banks as the pond level rose or by breaking through the blockage to generate lava surges downchannel. Small blockages commonly failed when the weight of the ponded lava exceeded the strength of the obstruction. At first, the dam would begin to creep downchannel, at increasing rates. Within several minutes, flow rates would increase from a few meters per minute to a few meters per second. Then the lava pond would break through a low or weak area to form a surge of lava down the channel. At times, this occurred in such volume that the released lava could not be contained in the channel below the dam (fig. 57.15). At other times, the rising impounded lava would lift and float the jammed debris over the constriction to form an overflow surge. When the volume of the breakout was reduced by overflows to an amount containable within the channel, the excess lava progressed down the flow as a channel surge.

Where the pond was confined behind high overflow levees, the weight of the pond could bulldoze the flank of the levee aside, widening the channel or causing failure of the levee. Failure of the levees, at times observed to open like a giant barn door, could abruptly release a large volume of lava along the flank of the flow rather than directly downchannel. Such lateral breakouts could generate major new lava tongues, such as flows 1A and 1B. In such breakouts large blocks of levee material were rafted downslope embedded in the overflow lava. Much of the volume of the eruption was dissipated in this way after March 29, causing slowing and stagnation of the flow terminus.

In lower reaches of the channel (transition zone), surges caused fluctuations of several meters in channel level; they also affected the height and rate of deformation of the marginal shear lenses adjacent to the channel. Increased marginal deformation during a surge was accompanied by creaking and crunching noises. The marginal shear areas rose during passage of a surge and subsided afterward, demonstrating that the zone of shearing was underlain by fluid lava hydraulically connected to the channel.

Flow velocities in the channel commonly increased during a surge, especially where the channel gradient was fairly uniform. Where the gradient flattened below a cascade, however, the effect of a surge was mainly to increase the lava level, with little or no increase in velocity. Many surges carried abundant debris from the causative blockage as a raft that spanned much of the channel and moved more slowly than the underlying lava. The cooler and more rigid rafted material tended to increase the bulk viscosity of the lava and drag along the marginal levees; these interactions raised the level of flow within the channel and decreased the velocity of the lava. A few minutes after passage of a surge, exceptionally fluid lava that had been stored in the interior of the blockage pond typically arrived in the channel; flow velocities increased, and the previous channel gradients were restored.

LEVEES

Marginal levees are common features of aa flows and are closely related to channel evolution (Hulme, 1974). At Mauna Loa in 1984, several types of levees formed that are broadly similar to those described for small short-lived aa flows on Mount Etna (Sparks and others, 1976). At Mauna Loa, however, levee growth varied notably with time and with position along the flow.

EARLY LEVEES

Early levees on Mauna Loa are represented by the broad topographically high rubbly flanks of the aa flow (fig. 57.9C: high points on the M-shaped profile) that were left behind in the zone of dispersed flow as the central zone of highest velocity flow drained downslope to form an incipient channel (fig. 57.5). In many places, lateral spreading of the flow tended to displace and cause outward avalanching of aa rubble along the early formed levees (fig. 57.9C). Thus, the early Mauna Loa levees seem transitional between the features that Sparks and others (1976) called initial levees and rubble levees. Nested lateral levees also tended to form rapidly at Mauna Loa, inside of the early lateral levees, as the center of the flow thinned and movement became concentrated along an incipient channel. In comparison with initial levees of aa flows on Etna, such early lateral levees on Mauna Loa aa flows were morphologically more complex, broader relative to channel width, had high points farther from the channel banks, and formed over a period of hours to days rather than within minutes of passage of the flow front. These differences seemingly reflect the larger size and longer movement history of the Mauna Loa flows. In addition, on Mauna Loa the flowing lava between the levees rapidly developed a concave-upward profile because of draining of the liquid flow core downslope and probably also because of effects of preexisting topography (fig.

A

FIGURE 57.15.—Channel overflows. ***A***, Begining of overflow at about 2,800-m level, at 1800 April 10. Blockage has broken, permitting ponded lava to spread downslope and overflow the channel. ***B***, Photograph taken about 5 minutes after that in *A*. Upper part of overflow has stagnated and lava is draining back into original channel; on lower slopes surge continues to flood and overflow channel.

57.9C) In contrast, profiles of flows on Etna (and also those modeled by Hulme, 1974), which are confined within marginal levees, are convex upward. On both volcanoes, formation of early levees appears related to the yield strength of the lava.

The early levees that formed at Mauna Loa were gradually modified by later processes of composite levee growth, mainly involving channel overflow and deformation of already formed levees. These processes produced complex levee structures somewhat similar to those described on Etna—accretionary, rubble, and overflow levees (Sparks and others, 1976)—although larger and more notably composite in origin. All levee growth on Mauna Loa flows, after a central channel was established, was caused by variations in channel level related to blockages and surges.

OVERFLOW LEVEES

The most common levee-building process was overflow of the channel banks during passage of surges. During vigorous surges, discrete small aa or pahoehoe flows spread laterally to produce overflow levees (figs. 57.16*A*, 57.9*D*, *E*) of the sort diagramed but not observed by Sparks and his associates. Weaker surges that completely filled the channel without overflowing caused scoriaceous or clinkery aa to accumulate along the channel margins, producing rapid growth in levee height by processes somewhat similar to the so-called accretionary levees described on Etna. Overflow and accretionary levee-building processes were thus intergradational, even during a single surge event. At Mauna Loa, levees formed by these

B

FIGURE 57.15—Continued.

surge-overflow processes had depositional slopes of no more than 10°–15°, in contrast to slopes of 50°–85° reported at Etna.

DEFORMATION LEVEES

An important process, which steepened overflow levees at Mauna Loa, was outward displacement of overflow levees pushed by the increasingly deep lava confined in the channel. By this mechanism, overflow levees with initial surface features of small lava flows were converted into angle-of-repose rubble ridges, which stood as much as 6–8 m above the original channel level (fig. 57.9*E*). At times, slabs of scoriaceous pahoehoe several meters across, derived from the crust of the channel lava, were tilted and overturned during upwelling of channel lava associated with surges (fig. 57.9*F*). These features are best described as deformation levees, although somewhat related in process and resultant appearance to the so-called rubble levees described near the toes of Etna flow fronts (Sparks and others, 1976). Deformation of a levee was commonly recognizable at a distance by rising dust clouds, as aa debris ground together and cascaded down the flank of the levee (fig. 57.16*B*). Such outward expansion was frequent during passage of surges, when channel levels were high, and was commonly accompanied by channel overflows, producing composite levee morphologies. The outward displacement of levees also caused fracturing, and at times lava from the interior of the channel oozed out along the base of the rubble levees. This process sometimes led to catastrophic failure of a levee flank, formation of a new lateral breakout, and draining of the lava ponded behind the levee.

Overflow and deformation levees did not form during early advance of the Mauna Loa flows; they constitute a distinct aspect of later evolution associated with blockages and ponding in the channel. Development of such levee features could provide a useful criterion to distinguish between long-lived and short-lived prehistoric aa flows.

ACCRETED LEVEES

Distinctive additional levee types, observed in the transition zone of the Mauna Loa flow system, are best termed accreted levees

A

B

FIGURE 57.16.—Lava levees, 1984 Mauna Loa eruption. ***A***, Overflow levee: channel level is low between surges. Slow overflows have produced shiny pahoehoe on levee flanks. Photographed on April 10, at about 2,800-m elevation. ***B***, Deformation levee: weight of perched lava channel is causing restraining levee to spread laterally, as indicated by dust clouds rising from blocks cascading down steepening levee flank. Result is angle-of-repose outer slopes of levees (see fig. 57.9*G*). Photographed on April 4, at 1,900-m elevation.

although different in origin and appearance from the accretionary levees of Sparks and others (1976). In the transition zone, characterized by a developing channel flanked by slowly moving lens-shaped ridges of aa rubble bounded by discrete shear zones (fig. 57.5), the initial levees were widened and enlarged by accretion of laterally moving rubble ridges. The ridges moved fairly rapidly during surges in the adjacent channel; during low stands of the channel, motion of the lateral ridges slowed, and some marginal ridges would accrete to stable flanking rubble levees. In many respects, this process provides a small-scale analog of plate-tectonic accretion of tectono-stratigraphic terranes (Jones and others, 1982). Some accreted levees originated as transverse pressure ridges near the flow toe, which were then deformed by continued flowage into U-shaped ridges (in plan view). These ridges subsequently were breached by continued movement within the center of the flow, and the limbs of the "U" became moving levees parallel to the channel margins (fig. 57.17).

POSTERUPTION CHANNEL PROFILES

During the eruption, channel depths were estimated mainly by reference to the half diameters of large lava boats (table 57.2). Once, we attempted to measure channel depths directly by dropping 5-m iron bars, stabilized vertically with streamers, from a helicopter. The channel center was difficult to hit by this technique, however, because radiative heat from the channel required a flight height of 100–200 m. Similarly, suitable locations for launching bars 2–3 m long in javelin fashion from high levees were rare, and such attempts failed to penetrate to the channel bottom.

After eruptive activity ceased, we measured profiles across the evacuated channels of flow 1, flow 1A, and the north flow at sites that had drained rapidly because of upflow beheading (fig. 57.18). Most profiles were at or near the flow-rate monitoring stations (fig. 57.1*B*), and some channel sites appeared unmodified except for draining of lava since our last monitoring measurements. Where the monitoring station had been modified by ponding or overflows, we profiled a nearby channel site that appeared representative of the geometry during the eruption. The posteruption channel profiles showed that most of the earlier depth estimates were 20–30 percent low, probably because the lava boats would first shoal on anomalously shallow reaches of the channel. Although the channel profiles improved our estimates of volume rates of flow, the measured depths are only minima because of residual ponded lava and rubble from caving levees. In addition, the profiles are of mature channels; channel geometry in earlier stages are inferred from observed changes in levee height and channel width during the eruption.

In addition to improving the volume calculations, the profiles show that the mature channel had (1) a remarkably uniform depth, about 6 m, from the vent to 17 km downflow; (2) a gradually increasing width downflow, especially within the transition zone (fig. 57.18*M*); and (3) an approximately rectangular shape. The bottoms of many channel profiles are near the projected pre-1984 surface, in agreement with the inference that still plastic parts of the initial flow material are eroded during deepening and narrowing of the maturing flow channel (fig. 57.9).

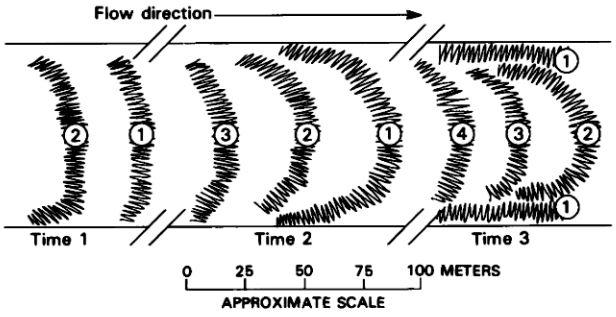

FIGURE 57.17.—Diagrammatic sketch (plan view) of formation, deformation, and accretion of pressure ridges to form accreted levees. Solid lines, margins of channel. Numbers identify individual sequentially formed pressure ridges.

TEMPERATURE AND DENSITY VARIATIONS OF LAVA

Key parameters in interpreting the evolution of the 1984 lava and channels are variations in lava temperatures and densities in relation to eruption duration, distance from vent, and lava type (table 57.1; fig. 57.19). Temperature determinations on the lavas were considered especially important for evaluating the hazard potential early in the eruption, because an increase in temperature might indicate the arrival of a more fluid magma batch from below the summit area.

LAVA TEMPERATURES

Temperatures were measured both directly by thermocouple probes inserted into accessible fluid lava and more remotely with a HOTSHOT 2-color infrared pyrometer aimed at active fountains or at brightly incandescant lava in standing waves in channels. Agreement among results by the two techniques was commonly within 5 °C when conditions were optimal. Some low measurments, deemed nonrepresentative and not plotted in figure 57.19, resulted from failure of the thermocouple to reach equilibrium before breakage of the probe tip, or from HOTSHOT measurement of fountains when the view included obstructing fume or cooler peripheral fallback material. Some equilibrium thermocouple measurements, which were lower than other values obtained from the same site, are thought to have inadvertently sampled cooler marginal lava. Details of measuring techniques and instrumental limitations are summarized in appendix 57.1.

The interpreted best measurements indicate that lava temperatures within a few hundred meters of the vents at about 2,850 m remained within the narrow range of $1,140 \pm 3$ °C throughout the eruption, varying little more than measurement uncertainties (fig. 57.19*A*). Temperatures measured on the most fluid lava at channel sites as much as 10 km downslope were only slightly cooler, in the

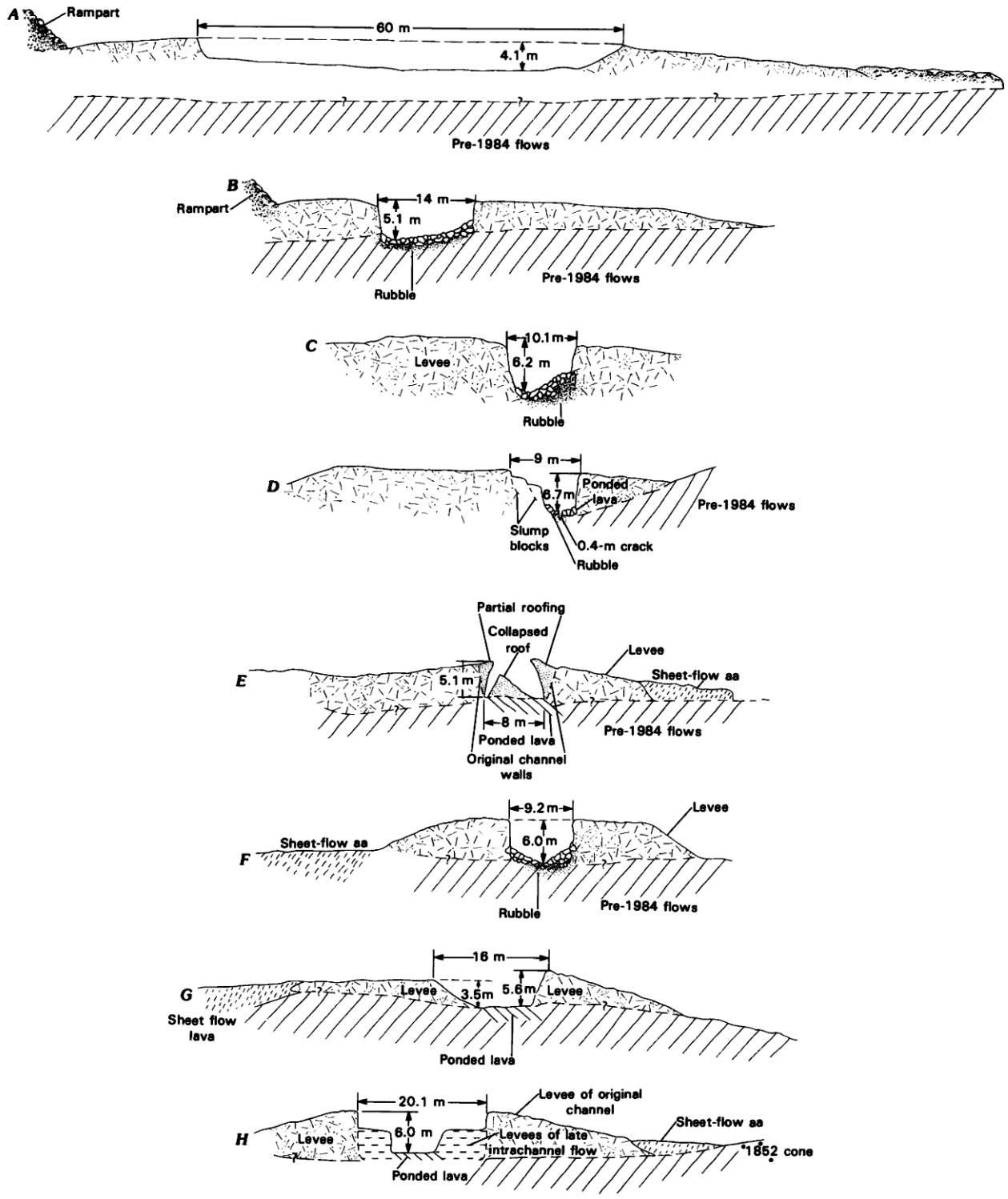
A
Rampart
60 m
4.1 m
Pre-1984 flows
B
Rampart
14 m
5.1 m
Rubble
Pre-1984 flows
C
Levee
10.1 m
6.2 m
Rubble
D
9 m
6.7 m
Ponded lava
Pre-1984 flows
Slump blocks
0.4-m crack
Rubble
E
Partial roofing
Collapsed roof
Levee
Sheet-flow aa
5.1 m
8 m
Ponded lava
Pre-1984 flows
Original channel walls
F
Sheet-flow aa
9.2 m
6.0 m
Levee
Rubble
Pre-1984 flows
G
16 m
Levee
3.5m
5.6m
Levee
Sheet flow lava
Ponded lava
H
20.1 m
Levee of original channel
6.0 m
Levee
Levees of late intrachannel flow
Sheet-flow aa
1852 cone
Ponded lava

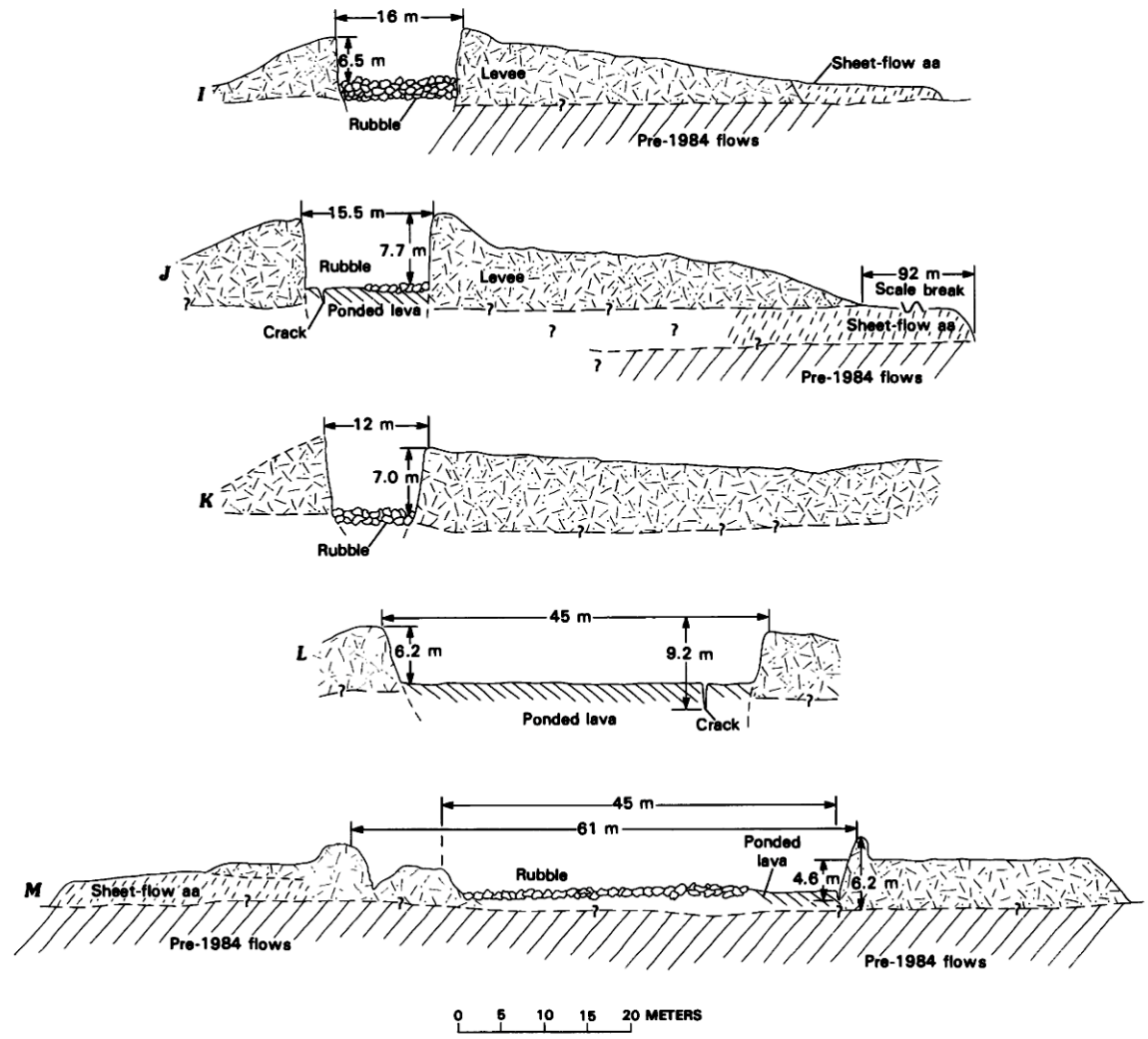

FIGURE 57.18.—Posteruption profiles (no vertical exaggeration) across channels of the 1984 Mauna Loa flows. Locations of channel stations shown on figure 57.1*B*. ***A***, Channel at about 2,900 m, 100 m downflow from westernmost vent, that was abandoned just after initial stabilization on about April 10. ***B***, Channel station 12, at about 2,900 m; mature stage of north channel, adjacent to vent rampart. ***C***, North flow, at 2,850-m elevation, 70 m from vent outlet. ***D***, Channel of north flow at 2,800-m elevation, approximately north of vent 2. ***E***, Channel station 10, at 2,720-m elevation; north flow, near monitor station. About 1 km from vent. ***F***, Channel at 2,710-m elevation, flow 1. About 2.5 km from vent. ***G***, Channel at 2,550-m elevation, flow 1; probably a channel formed after April 8. About 3.5 km from vent. ***H***, Channel station 8; 2,540-m elevation, flow 1; pre-April 8 channel, just above monitor station. About 4 km from vent. ***I***, Channel station 7, 2,200-m elevation, flow 1; pre-April 8 channel, near monitor station. About 6.5 km from vent. ***J***, Channel station 4, 1,950-m elevation, flow 1; pre-April 8 channel, near monitor station. About 10.5 km from vent. ***K***, Channel station 3, 1,800-m elevation, flow 1; pre-April 8 channel, near monitor station. About 12 km from vent. ***L***, Channel at 1,800-m elevation, flow 1; pond below channel station 3. About 12.5 km from vent. ***M***, Channel station 1, 1,600-m elevation, flow 1A; pre-April 8 channel, near monitor station. About 15 km from vent.

TABLE 57.1.—*Lava temperature and density, 1984 Mauna Loa eruption*

[Days, time in days from beginning of eruption; distance, distance from vent]

Location	Date (mo/d)	Time (H.s.t.)	Days	Elevation (m)	Distance (km)	Temperature (°C)	Code[1]	Density (g/cm³)	Sample	Comments
3,500-m vents	3/25	1015	0.37	3,500	0.01	1,073	T 1 B I	0.85	NER–7	Channel at vent; couldn't probe below surface; poor reading.
SE. flow, terminus	3/25	1540	.59	2,670	6.6	1,128	T 2 B E	2.23	NER–1F	Aa flow front; imbedded 2 m in soft core; stable 15 min.
Flow 1	3/25	--	.70	2,560	3.6	--		1.29	4/18NB1	Aa, core of sheetwash flow.
Vent 1, middle	3/26	0828	1.29	2,910	.0	1,125	H P	--	--	Fountain; tripod rest, 50 m distance.
Do.	3/26	0854	1.31	2,910	.0	1,145	H G	--	--	Fountain; tripod rest, 50 m distance; stable 1,144–1,145 °C.
Vent 1, east end	3/26	1058	1.40	2,890	.0	1,103	T 1 B F	1.08	NER–12/2	1-m-thick spatter-fed flow; failed tip several tries.
Do.	3/26	1324	1.50	2,890	.0	1,146	H G	1.20	NER–12/3	Fountain, tripod at 20 m; stable 1,134–1,146 °C, observer 1.
Do.	3/26	1340	1.51	2,890	.0	1,147	H G	--	--	Fountain, tripod at 20 m; stable 1,134–1,146 °C, observer 2.
Flow 3	3/26	1420	1.54	2,860	.0	1,131	T 1 B E	1.19	NER–12/13	Pahoehoe overflow from main channel; stable 2 min.
Flow 1	3/26	1600	1.61	2,760	1.5	1,139	T 1 B G	1.18	NER–12/4	Directly in main channel; stable several minutes.
Vent 1, east end	3/26	1613	1.62	2,890	.0	--		.92	NER–12/14	Spatter.
Flow 1	3/26	1730	1.67	1,880	11.7	1,131	T 2 B E	1.77	NER–12/5	Overflow 30 m from channel; stagnating when measured.
Vent 1, main vent	3/27	--	2.50	2,890	.15	--		.60	NB1ML84	Cooled shelly pahoehoe overflow from main channel.
Vent 1, middle vent	3/27	1421	2.54	2,910	.01	1,131	T 1 B E	.83	NER–12/12	Spatter-fed flow; 60 cm thick; stable 0.5 min.
Vent 1, main vent	3/27	1435	2.55	2,500	.0	1,139	H G	--	--	Fountain, tripod rest; 10–15 m distance; stable 1,135–1,139 °C.
Do.	3/27	1545	2.60	2,890	.0	1,139	H G	--	--	Do.
Do.	3/27	2016	2.79	2,890	.01	1,131	T 1 B E	.98	NER–12/15	Spatter-fed flow; 1 m thick; stable 0.5 min.
Do.	3/27	2035	2.80	2,890	.0	1,140	H G	1.12	NER–12/16	Fountain, tripod rest; 10–15 m distance; stable 1,135–1,140 °C.
Do.	3/27	2350	2.93	2,890	.02	1,135	T 1 B G	1.36	NER–12/17	Tube, directly from vent; stable 3 min.
Do.	3/28	0610	3.20	2,890	.02	1,137	T 1 B G	.92	NER–12/18	Do.
Vent 4	3/28	0835	3.30	2,810	.05	1,128	T 1 B E	.92	NER–12/10	Tube emitted directly from vent pond; stable.
Do.	3/28	1241	3.47	2,810	.0	1,131	T 1 B E	--	NER–12/20	Do.
Do.	3/28	1610	3.61	2,810	.05	1,128	T 1 B E	--	NER–12/21	Do.
Flow 1A	3/29	1300	4.50	1,610	16.50	--		2.6	--	Core of aa flow.
Vent 4	3/29	1755	4.69	2,810	.0	1,136	T 1 B G	1.19	NER–12/23	Top of west hornito; 2 times; stable 3 and 2 min.
Do.	3/30	0656	5.23	2,810	.0	1,130	T 1 B E	--	NER–12/24	Tube emitted directly from vent pond; stable.
Do.	3/30	0840	5.30	2,810	.0	1,135	T 1 B G	1.84	NER–12/25	Top of west hornito; stable 3 min.
Flow 1A	3/30	1230	5.46	1,370	20.4	1,103	T 2 B F	--	--	Horizontal into lobe terminus; >20 cm penetration, poor.
Do.	3/30	1420	5.54	1,750	14.2	1,126	T 2 B E	--	NER–12/28	Slabby pahoehoe overflow 30 m from channel; flow stangnant.
Vent 4	3/30	1647	5.64	2,810	.0	1,136	T 1 C G	1.02	NER–12/26	Short tubed flow from west hornito; stable 5 min.
Flow 1A	3/31	0712	6.21	1,150	24.5	1,086	T 2 B F	--	--	Flow terminus; >30 cm penetration; poor reading.
Do.	3/31	1056	6.40	1,610	16.5	1,125	T 2 B F	--	--	Overflow 3 m from active main channel; aborted before stable.
Do.	3/31	1250	6.48	1,950	10.2	1,133	T 1 B G	1.22	NER–12/29	Tube, branch of main channel.
Vent 4	3/31	1556	6.60	2,810	.0	1,132	T 1 B E	--	--	Short tubed flow from west hornito; stable 5 min.
Do.	3/31	1630	6.64	2,810	.0	1,133	T 1 B E	1.01	NER–12/30	Do.
Do.	4/01	1154	7.44	2,810	.0	1,129	T 1 B E	--	NER–12/31	Tube emitted directly from vent pond; stable.
Vent 1, main vent	4/02	1000	8.36	2,890	.03	1,135	T 1 B E	1.20	NER–12/32	Tube emitted directly from vent; stable 4 min.
Do.	4/02	1047	8.39	2,890	.00	--		.79	NEW–12/32	Spatter.
Vent channel	4/02	1155	8.44	2,860	.15	1,137	H G	--	--	Underside of standing wave; 15 m distance; tripod rest, stable.
Vent 1, main vent	4/02	1645	8.64	2,890	.07	1,136	T 1 B G	1.10	NER–12/34	Tube emitted directly from vent; stable 2 min.
Do.	4/02	1715	8.66	2,890	.00	--		.70	NER–12/35	Spatter.
Do.	4/03	1012	9.37	2,890	.12	1,133	T 1 B E	--	NER–12/36	Tube emitted directly from vent; stable.
Do.	4/03	1230	9.54	2,890	.12	1,140	T 1 B G	--	NER–12/37	Do.
Do.	4/03	1417	9.54	2,890	.12	1,138	T 1 B G	--	NER–12/38	Do.
Do.	4/04	0830	10.10	2,890	.03	1,141	T 1 B G	2.40	NER–12/40	Tube emitted directly from vent; stable 5 min.
Do.	4/04	0915	10.33	2,890	.0	--		.51	NER–12/41	Tube emitted directly from vent.
Do.	4/04	1545	10.60	2,890	.12	1,139	T 1 B G	1.41	NER–12/39	Tube emitted directly from vent; stable.
Do.	4/04	1550	10.60	2,890	.05	1,140	T 1 B G	1.54	NER–12/42	Tube emitted directly from vent; stable 5 min.
Do.	4/05	1230	11.46	2,890	.3	1,139	T 1 B G	--	NER–12/43	Tube emitted directly from vent.
Vent 4	4/06	0945	12.35	2,810	.02	1,131	T 1 B E	.82	NER–12/45	Tube emitted directly from western hornito; stable 2 min.
Do.	4/06	1000	12.36	2,810	.0	--		1.00	NER–12/46	Spatter from western hornito.
1852 vent station	4/06	1220	12.45	2,500	4.0	1,128	T 1 B I	1.15	NER–12/47	Directly in main channel; never stable.
Flow 1A	4/06	1430	12.55	1,940	11.0	1,133	T 2 B G	1.72	NER–12/48	Aa overflow from main channel; 2 m thick; stable 5 min.
Vent 4	4/06	1630	12.63	2,810	.02	1,140	T 1 B G	.80	NER–12/49	Tube emitted directly from western hornito; stable 2 min.
Flow 1	4/07	--	13.5	2,240	6.8	--		2.57	4/18NB3	Cooled aa levee material.
Vent 1, main vent	4/07	1405	13.53	2,890	.3	1,142	T 1 B G	1.83	NER–12/44	Tube emitted directly from vent; stable.
Do.	4/07	1053	13.39	2,890	.1	1,140	T 1 B G	.89	NER–12/50	Do.
Vent 4	4/07	1650	13.64	2,810	.10	1,124	T 1 B E	1.15	NER–12/51	Do.
Do.	4/07	1730	13.67	2,810	.1	1,121	T 1 B F	--	NER–12/52	Tube emitted directly from vent pond; stable.
1852 vent station	4/08	1026	14.38	2,500	4.0	1,100	T 1 B F	.99	NER–12/53	Directly in main channel; never stable.
Vent channel	4/08	1145	14.43	2,880	.15	--		.53	NER–12/54	Pahoehoe overflow from main channel.
Flow 1	4/08	1306	14.49	2,230	6.0	--		1.25	NER–12/57	Overflow from main channel.
Do.	4/08	--	14.5	1,980	10.2	--		2.31	4/18NB4	Cooled lava ponded in beheaded channel.
North flow	4/08	1445	14.56	2,930	2.5	1,123	T 1 B F	--	NER–12/58	Overflow from channel, never stable.
North flow vent	4/08	1515	14.58	2,910	.15	1,122	T 1 B F	.69	NER–12/55	Pahoehoe overflow from main channel; never stable.
North flow	4/08	1530	14.59	2,930	.1	--		.38	NER–12/56	Scoop sample from channel.
North flow vent	4/08	1620	14.62	2,910	.20	1,126	T 1 B E	--		Pahoehoe overflow from main channel; stable 2 min.
Flow 1	4/09	--	15.5	2,550	3.3	--		1.43	4/18NB2	Cooled lava ponded in beheaded channel.
North flow channel	4/11	0850	17.31	2,930	.0	--		.51	NER–12/60	Spatter, stable.
Do.	4/11	1500	17.57	2,930	.0	--		.33	NER–12/62	Spatter.
Do.	4/11	0850	17.31	2,930	.0	--		.51	NER–12/60	Spatter, stable.
Do.	4/11	1500	17.57	2,930	.0	--		.33	NER–12/62	Spatter.
Do.	4/11	1610	17.61	2,930	.04	1,087	T 1 B I	.54	NER–12/63	Scoop sample from channel; never stable.
Vent 9,146 station	4/11	1700	17.65	2,700	2.6	1,125	T 1 B E	--		Pahoehoe overflow from main channel; stable 2 min.

TABLE 57.1.—*Lava temperature and density, 1984 Mauna Loa eruption—Continued.*

Location	Date (mo/d)	Time (H.s.t.)	Days	Elevation (m)	Distance (km)	Temperature (°C)	Code[1]	Density (g/cm³)	Sample	Comments
Do.	4/11	1710	17.66	2,700	2.6	1,106	T 2 B F	--		Aa overflow from main channel, stable 2 min.
Vent 1, main vent	4/13	0935	19.34	2,890	.20	1,102	T 1 B F	.73	NER-12/64	Directly in main channel; never stable.
Do.	4/13	1008	19.36	2,890	.10	1,132	T 1 B E	2.12	NER-12/61	Tube emitted directly from vent; never stable.
Vent 1, west vents	4/13	1142	19.42	2,930	.03	1,125	H P	--		Fountain; hand held; 20 m distance over channel; poor reading.
North flow	4/13	1215	19.45	2,900	.16	1,137	T 1 B G	.83	NER-12/65	Tube from ponded channel; stable 2 min.
Vent 4	4/13	1550	19.60	2,810	.01	1,121	T 1 B I	.57	NER-12/xx	Tube emitted directly from vent.
North flow channel	4/14	0945	20.35	2,930	.15	1,122	T 1 B I	.89	NER-12/66	Overflow from channel; never stable.

[1]Meaning of code symbols:
1, Thermocouple measurement, small-gauge (1.5-mm-diameter) wire.
2, Thermocouple measurement, large-gauge (6-mm-diameter) wire.
B, Thermocouple wires exposed to lava.
G, Grounded thermocouple; wires sheathed with INCONEL stainless steel.
E, Thermocouple measurement; stable temperature in equilibrium with lava but in geologically unfavorable site (thin flow, stored lava, and so on).
F, Failed thermocouple measurement; probe broken before equilibrium temperature achieved.
G, Good measurement; stable temperature in a geologically good site (thermocouple), or with good atmospheric conditions (HOTSHOT).
H, Measurement by two-color HOTSHOT infrared pyrometer.
I, Thermocouple became sheathed with a lava icicle before equilibrium temperature was achieved.
P, HOTSHOT measurement under poor atmospheric conditions.
T, Thermocouple measurement.

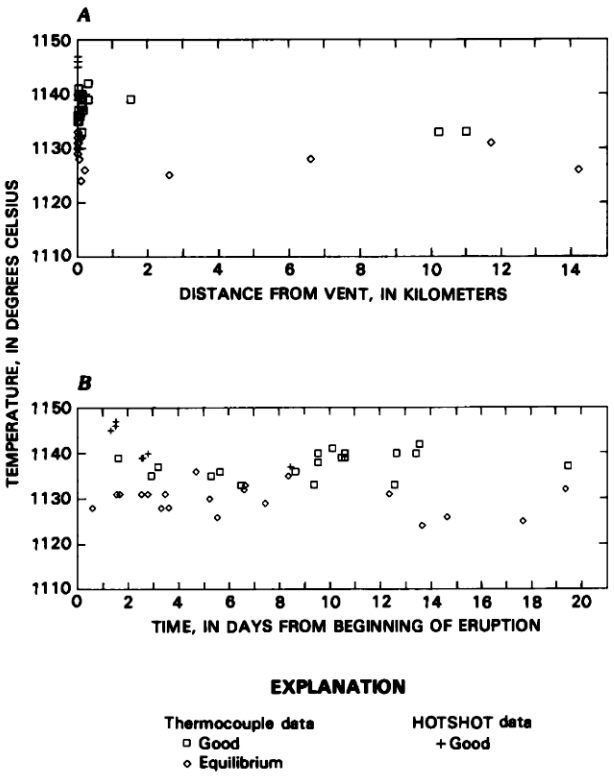

FIGURE 57.19.—Measured lava temperature in 1984 Mauna Loa eruption. Includes all good or equilibrium data, thermocouple and HOTSHOT techniques. Good values are from superior sites, as ranked on geologic criteria; equilibrium thermocouple data are stable results from less favorable sites. Temperature data are from table 57.1; measurement techniques and limitations are described in appendix 1. ***A***, Temperature plotted against distance from eruptive vent; values by the same technique are at most about 5 °C higher at the vent than downchannel. ***B***, Temperature plotted against time: no sigificant variation is evident.

range of 1,135 ± 5 °C. Most of the infrared-pyrometer temperatures for fountains were a few degrees hotter than the best near-vent lava temperatures.

Temperatures from small-volume shield-building lava of the lowest vent (4), at 2,785-m elevation, at times approached 1,140 °C but typically were 5–10 °C cooler. These temperatures are thought to be lower because some vent 4 lava was fed through a lava tube from vent 3, a few hundred meters uprift. The presence of tube-fed lava in this shield was initially inferred from the low to non-existent fountains at vent 4, lower temperature and higher density of spatter and lava from vent 4 compared to those of vent 1 (the main upper vent), and development of a lava tube from vent 3 along the north edge of vent 4 during the first few days of activity. Presence of a lava tube during later vent 4 activity was confirmed by its collapse at the end of the eruption on April 14.

Temperatures obtained at vent 1 are believed to approximate the eruption temperature, as indicated by the consistent results by both measurement methods and the lack of variation during the 20 days of the eruption (fig. 57.19*B*). The vent temperatures for the 1984 Mauna Loa eruption are similar to temperatures measured by the same techniques during recent Kilauea eruptions in which aa flows were dominant (1,135–1,145 °C; Ulrich and others, 1984). These eruption temperatures are 20–30 °C below the expected one-atmosphere liquidus temperature of the lava, as indicated by experimental determinations for other Hawaiian tholeiite (Yoder and Tilley, 1962).

Temperatures of the Mauna Loa flows are about the same as those from most thermocouple measurements for Kilauea eruptions over the past 30 years. Higher temperatures reported for Kilauea lavas and fountains are optical pyrometer measurements that were corrected upward for atmospheric absorption (Alt and others, 1961; Wright and others, 1968), except for the temperatures of 1,500–1,165 °C measured by Swanson (1973) through skylights in lava tubes of pahoehoe from Mauna Ulu. More data are needed to evaluate whether higher eruption temperatures are associated with

long-traveled tube-fed pahoehoe flows, such as have characterized many prehistoric Mauna Loa eruptions.

LAVA DENSITIES

Vesicularity of the 1984 lava was noted in the field to decrease downchannel, as discussed in connection with the variations in lava types. Near the vent outlet, channel lava was fluffy near-reticulite that had the consistency of whipped egg white; downflow, it became dense blocky lava, containing only the scattered irregular vesicles typical of consolidated aa (Macdonald, 1972, p. 70). Density measurements on samples collected at temperature sites confirm a downflow increase in density (fig. 57.20), particularly for samples collected during a single day, and also indicate a gradual decrease in density of vent material during the eruption (fig. 57.21).

The increase in density of lava with distance from the vent (fig. 57.20*A*) is striking, when differing lava types are distinguished. At the vent, the densest values are largely for degassed pahoehoe oozed out from small tubes near the base of the spatter ramparts or from the quietly effusive vent 4 (fig. 57.20*A*, triangles). In contrast, quenched spatter and frothy lava dipped from the channel have densities as low as 0.35 g/cm^3, indicating about 85 percent porosity. Downchannel, samples from the incandescent cores of aa flow fronts are denser than those from rapidly quenched channel overflows (typically scoriaceous aa) or samples taken directly from the channel. These changes in density must relate to degassing and kneading out of vesicles in the lava as it flowed downchannel. Significant gas emission from the channel lava was evident in the field; SO_2 levels were so high that manned observations were rarely feasible downwind of the channel. The downchannel density changes probably contributed significantly to the decreased downchannel lava volumes measured in the 1984 channel system, as discussed later.

In addition to density changes with distance from the vent, the density of spatter sampled at the vent decreased fairly systematically during the eruption, from 1.0–1.2 g/cm^3 early in the activity at the 2,900-m vents to about 0.5 g/cm^3 late in the eruption (fig. 57.21*A*). We interpret this trend as reflecting an increasing ratio of gas to magma in the fountains as discharge rate declined during the eruption. Temporal changes in density of channel or overflow samples were more subdued, presumably because such effects were masked by large concurrent effects of downchannel degassing (fig. 57.21*B*).

The long-term decrease in spatter density is in accord with the observed inverse correlation between fountain height and channel level at the vent, which involved fluctuations over intervals of a few tens of minutes to a few hours (fig. 57.22). At the times of higher fountains, which yielded the least dense and most gas-rich spatter—at times approaching reticulite—the channel level dropped, indicating a decrease in bulk eruption rate of lava. Alternatively, more gas may have been exsolved and kneaded out during the high-fountain phases, producing denser channel lava and lower channel levels without a decrease in discharge. Similar general effects have been noted at several eruptions of Kilauea, in which high wispy fountaining (maximum gas release) occurs as lava production declines just before the end of the eruption (Swanson and others, 1979; Moore and others, 1980).

RELATION OF LAVA TEMPERATURE, VESICULARITY, AND VISCOSITY

The temperature measurements and other observations on Mauna Loa lava bear significantly on interpretations that the pahoehoe-aa transition reflects increased viscosity related to gradual downflow cooling in open channels (Swanson, 1973; Peterson and Tilling, 1980). At Mauna Loa, lava temperatures varied little for 10 km downstream from the vent (fig. 57.19*A*). Downflow temperatures have been similarly stable in aa at Kilauea Volcano (fig. 57.23). Bulk aa temperatures were presumably lower downflow than near the vent, because the ratio of fluid melt to pasty clots and solid debris decreased down the active channel. Some process, however, maintained the temperature of the fluid portion of the aa, and the bulk aa viscosity increased independently of the limited temperature variations in the fluid part of the channel fill.

High temperatures in the aa were partly sustained by heat of crystallization, as indicated by a downflow increase in microlite population (see next section). Frictional deformation of the melt (Shaw, 1969, p. 532) may also have been significant. Lava in the channel had the consistency of reticulite near the vent, and even 20 km from the vent it contained 30 volume percent vesicles. The melt fraction was present in the form of vesicle walls that deformed as the lava degassed and flowed turbulently downchannel. Flexing of bubble walls (during flowage, turbulent mixing, and buoyant rise of gas), supplemented by friction along margins and shear planes within the channel, is thought to have contributed significant heat to maintain high temperatures in the channel lava.

Given that temperatures in the fluid-melt component were stable and that the slope gradient and flow velocity decreased downflow, what produced the observed increase in viscosity and initiated the downflow transition to aa? On April 2, the apparent viscosity in the channel near the vent was about 10^2 Pa·s; at 1,950 m, pahoehoe channel fill had an apparent viscosity of 10^3 Pa·s; and at 1,600 m, the apparent viscosity of aa channel fill was about 10^5 Pa·s, as determined by relations between flow velocity, channel gradient, and channel depth (Moore, chapter 58). The observed increase in both microlite content and solid debris downflow must have increased the viscosity of the silicate fraction (Shaw, 1969, fig. 2). In addition, the viscosity increases appear closely related to density increases in the channel lava (fig. 57.20). The density increases require an attendant decrease in gas and vesicle content of the channel lava and increased thickness of vesicle walls. Decreased vesicularity has been shown experimentally to increase the viscosity of lava (Murase, 1962; Shaw and others, 1968). Thus, even at constant melt viscosity, the *bulk* viscosity of the channel lava would increase without changes in temperature or microlite population. Thicker vesicle walls would also increase resistance to flexing of the melt, reduce associated deformational heating, and eventually allow a negative heat budget.

High gas content and thin vesicle walls may, in part, also account for the low viscosity and high fluidity of pahoehoe.

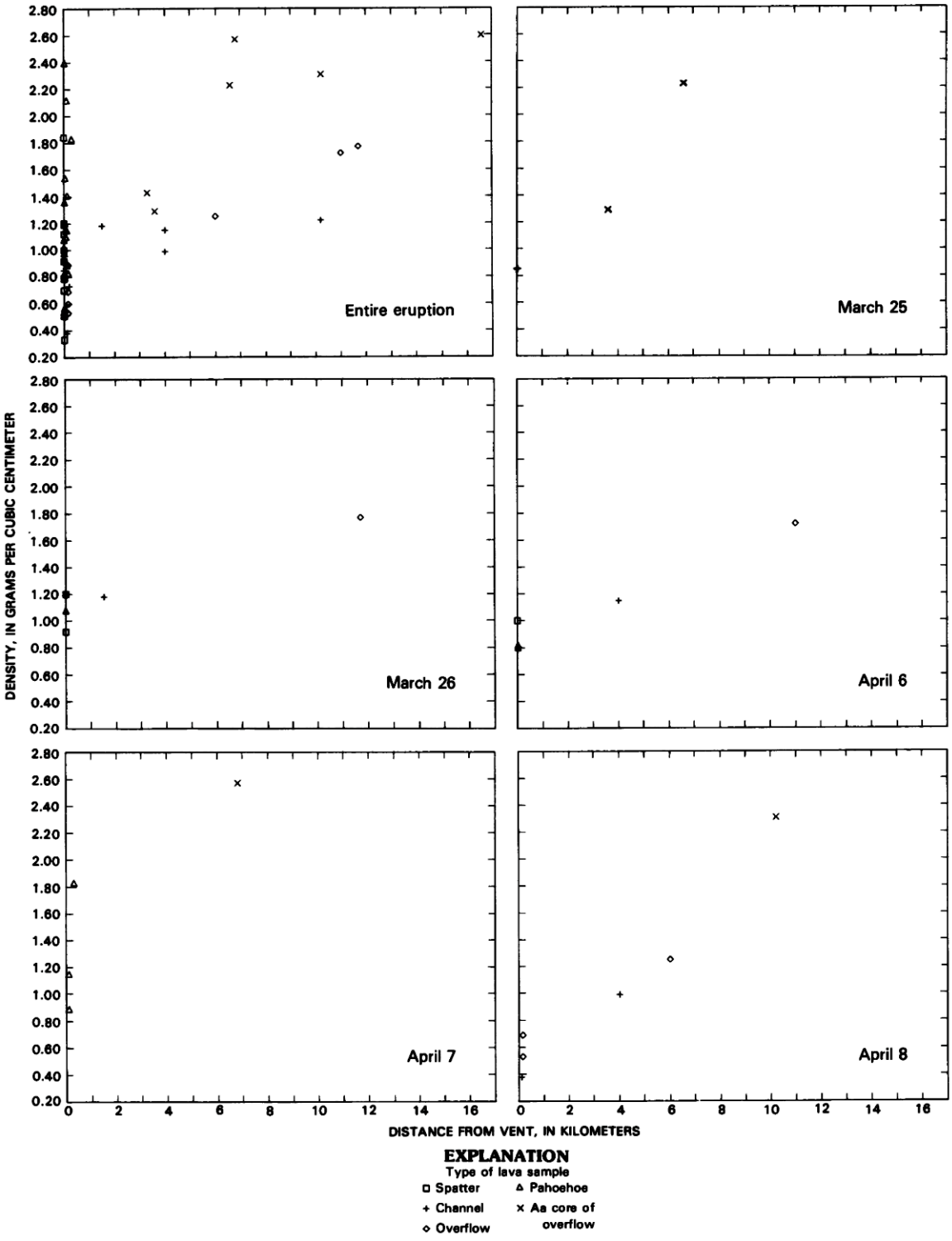

FIGURE 57.20.—Measured lava density plotted against distance from the vent, 1984 Mauna Loa eruption. Data, shown for individual dates as well as for entire eruption, are from table 57.1. All samples were collected hot and quenched in water. Density was determined by weighing a measured cube, sawn from the interior of sample, that had been dried at 20 °C.

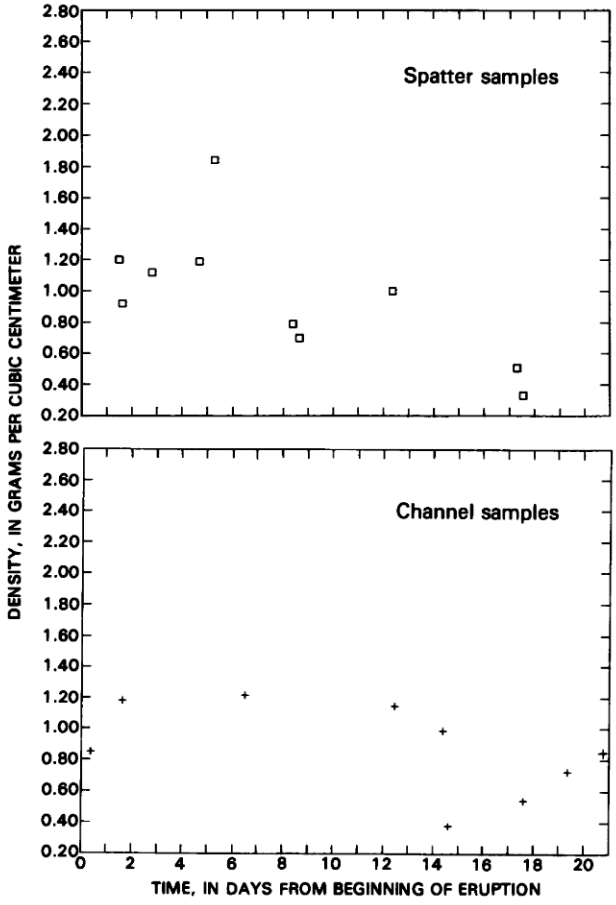

FIGURE 57.21.—Measured lava density of spatter samples and channel samples plotted against time. Data are from table 57.1.

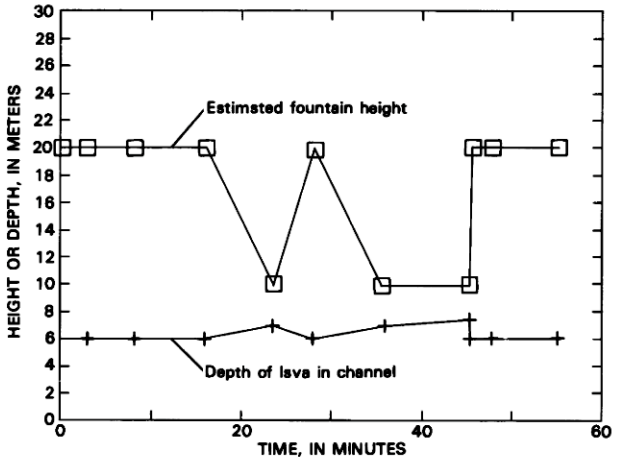

FIGURE 57.22.—Variation of lava level in channel versus height of the fountains at the main vent. Data obtained around 1200 on April 2, 1984. Fountain heights were visually estimated by reference to surveyed height of spatter rampart.

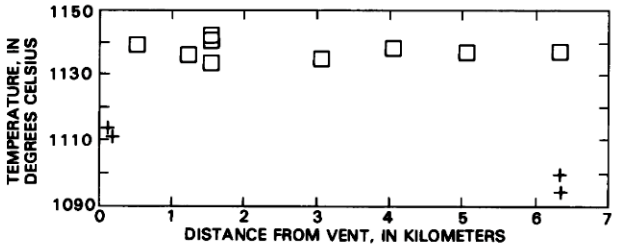

FIGURE 57.23.—Temperature plotted against distance of travel for Kilauea aa flows from the 1983–84 east-rift-zone eruptions. Plus, sample from phase 9, southeast flow; square, sample from phase 16, southeast flow.

Pahoehoe is more vesicular than aa, and retarded degassing in lava tubes may delay the transition to aa, along with the insulating role of the tube (Swanson, 1973). During the Mauna Loa eruption, pahoehoe in tubes flowed at velocities only about 20 percent slower than in open channels. The tubes formed along channels where flow was laminar and flow rates were fairly low and steady or decreasing. In high-volume channels, incipient roofs of tubes were continually broken up and rafted away. Slower flow in the tubes was promoted by lower eruptive volume and by drag against the roof. The slow flow rate appears to have favored less turbulent flow; it thus retarded stretching and breaking of vesicles, maintaining a lower bulk viscosity. The higher vesicle population also may have (1) allowed more rapid flexing of the vesicle walls, (2) generated deformational heating farther from the vent, and (3) combined with the insulating properties of the tube (Swanson, 1973), retarded formation of pasty clots and delayed viscosity increases.

Observations during temperature measurements (see app. 57.1) demonstrate an interrelation between vesicularity and viscosity. A lava sheath invariably formed on even the small-gauge thermocouple if the pahoehoe was moving more than about 0.5 km/h and lava was allowed to flow past the thermocouple tip. The observer could stop growth of the lava sheath by walking the tip downflow with the lava at velocities up to about 3 km/h. At higher flow velocities, the temperature measurements invariably terminated with a thermocouple sheathed in lava. The sheaths were denser than the channel fill and had the consistency of thick taffy, similar to lava from cores of aa flows much farther from the vent, where inserting a probe required more effort.

Two observations suggest that the lava sheath resulted from breakage of vesicle walls and adherence of the viscous melt, rather than from freezing of the melt against the probe. First, the size and growth rate of the lava sheath correlated with velocity of the flowing

lava: the faster the flowage past the thermocouple, the larger were the lava sheaths. Second, thermocouples were carefully preheated prior to insertion, particularly when measuring flowing lava, yet probes in flowing lava accumulated a sheath while those in motionless lava did not. We infer that the thermocouple stretches and breaks the gas bubbles in moving lava, increasing the bulk viscosity of the adjacent melt and making additional melt available to adhere to the probe. The growing surface area exerts additional drag on adjacent melt, hastens bubble breakage, and causes faster accumulation of melt on the sheath.

LAVA CRYSTALLINITY

Increases in crystallinity affected flow rheology of the 1984 lava both over time at the vents and during flow down the lava channel. Three discrete textural populations of crystals are present: (1) sparse resorbed phenocrysts or xenocrysts of magnesian olivine as much as 5 mm in diameter; (2) dusty microlites less than 0.01 mm in size; and (3) microphenocrysts of augite, plagioclase, and olivine commonly 0.05–1.0 mm in length.

The sparse olivine phenocrysts everywhere are less than 0.5 percent of the lava, did not vary in abundance significantly during the eruption, and are interpreted as disequilibrium crystals that were present in the summit magma reservoir before eruption. Microlites are absent in vent spatter and become increasingly abundant in quenched downchannel samples; they record late groundmass crystallization of the lava as it flowed down the channel. Such surface crystallization of channel lava is probably largely responsible for the observed progression of flowage zones (fig. 57.5), but it seems to have occurred uniformly throughout the eruption. In contrast, the content of microphenocrysts in quenched spatter increased strikingly during the eruption, from less than 0.5 percent of the lava during initial summit activity to as much as 30 percent during the waning eruptive phases (figs. 57.24, 57.25*A*). Microphenocryst size increased concurrently with abundance (fig. 57.25*B*), although the precision of measurement is lower. Microphenocryst size and abundance increased rapidly during the first few days of the eruption, slowed during the subsequent two weeks, and increased slightly again late in the eruption (fig. 57.25). Large changes occurred within a few hours after beginning of the eruption on March 25, as the vents migrated from the summit region downrift to the 2,900-m level, but the abundance and size of microphenocrysts continued to increase after the main vent site stabilized. These changes occurred in the lava before its eruption, as documented by quenched spatter samples, although the same microphenocryst populations are readily recognized in downchannel samples despite additional crystallization of microlites during surface flowage.

During these changes, bulk major-oxide compositions remained constant virtually within analytical uncertainty (table 57.2; Lockwood and others, 1985). This compositionally uniform 1984 lava is in marked contrast to lava erupted during Kilauea rift activity (Wright and Fiske, 1971; Garcia and others, 1984) but is typical for Mauna Loa rift eruptions (Rhodes, 1983).

Most microphenocrysts in the 1984 Mauna Loa lava occur as skeletal, intergrown, and radiating blades and plates (fig. 57.24), including elongate, cored, and swallow-tailed shapes that are typical of rapid crystallization from undercooled liquids (Walker and others, 1976; Lofgren, 1981). Such undercooled textures are especially prevalent in the phenocryst-poor lava of early eruptive phases; late eruptive phases have textures indicative of more prolonged equilibrium crystallization. We attribute the growth of microphenocrysts characterized by undercooled textures largely to separation of a gas phase during the eruption, not to a decrease in magma temperatures.

Observed eruptive temperatures remained constant at 1,140 ± 3 °C (fig. 57.19*B*), which is 20–30 °C below calculated liquidus temperatures for most phases at one atmosphere (olivine 1,186 °C, plagioclase 1,169 °C, and clinopyroxene 1,146 °C, all ±15 °C; method of Nielson and Dungan, 1983). The observed lava temperatures would approximately coincide with the liquidus if the pre-eruptive magma contained about one percent volatile content (Yoder and Tilley, 1962). A pre-eruptive volatile content of about 0.5 percent has been calculated from gas data for tholeiitic basalt from Kilauea Volcano (Greenland and others, 1985), and about one percent volatiles is the estimated average for tholeiitic basalt in general (Haggarty, 1981).

The virtual absence of microphenocrysts in much of the lava erupted early on March 25, followed by increases in the number and size of microphenocrysts (figs. 57.24, 57.25), suggests that the magma reservoir below the summit was initially sufficiently pressurized by volatiles to lower the liquidus temperature to about 1,140 °C, thereby inhibiting crystallization. With depressurization of the magmatic system beginning at onset of the eruption, separation of gas undercooled the magma without actually lowering the observed lava temperatures, thereby inititiating precipitation of microphenocrysts. Degassing at the summit began at onset of the eruption and was later focused at the 3,550-m level, uprift of the active lava vents (Casadevall and others, 1984).

Even slight undercooling can have profound effects on the nucleation and growth rates of crystals. At 20–30 °C of undercooling, crystals in basaltic melts can grow to sizes of 1 mm within periods as brief as a few hours (Kirkpatrick, 1976, 1977). The only alternative to growth of microphenocrysts during the eruption—a zoned pre-eruption magma chamber—seems less able to account for the compositional uniformity of the erupted lava or its undercooled quench textures.

The volatile loss needed to initiate crystallization may have been small. Before eruption, basaltic magmas in the shallow reservoirs beneath the summits of Mauna Loa and Kilauea are believed to contain <0.2 percent CO_2, 0.2–0.3 percent H_2O, and 0.1 percent S (Moore, 1965; Greenland and others, 1985; Greenland and others, in press). Because of their relative solubilities, S and CO_2, but not H_2O, would have separated from the magma during transit from the summit reservoir down the rift zone to just below the vent. If the rift magma was under lithostatic confining pressures, H_2O may have saturated and begun to separate only at depths as shallow as 100–200 m below the surface. Although confining pressures within the upper kilometer of the fractured rift zones of Hawaiian volcanoes are unlikely to be purely lithostatic, and may at times approach atmospheric, these relations nevertheless cast doubt on the ability of H_2O loss alone to account for the undercooling and crystallization of the 1984 magma. High flow rates of the rift magma, efficient degassing, and rapid crystallization would be

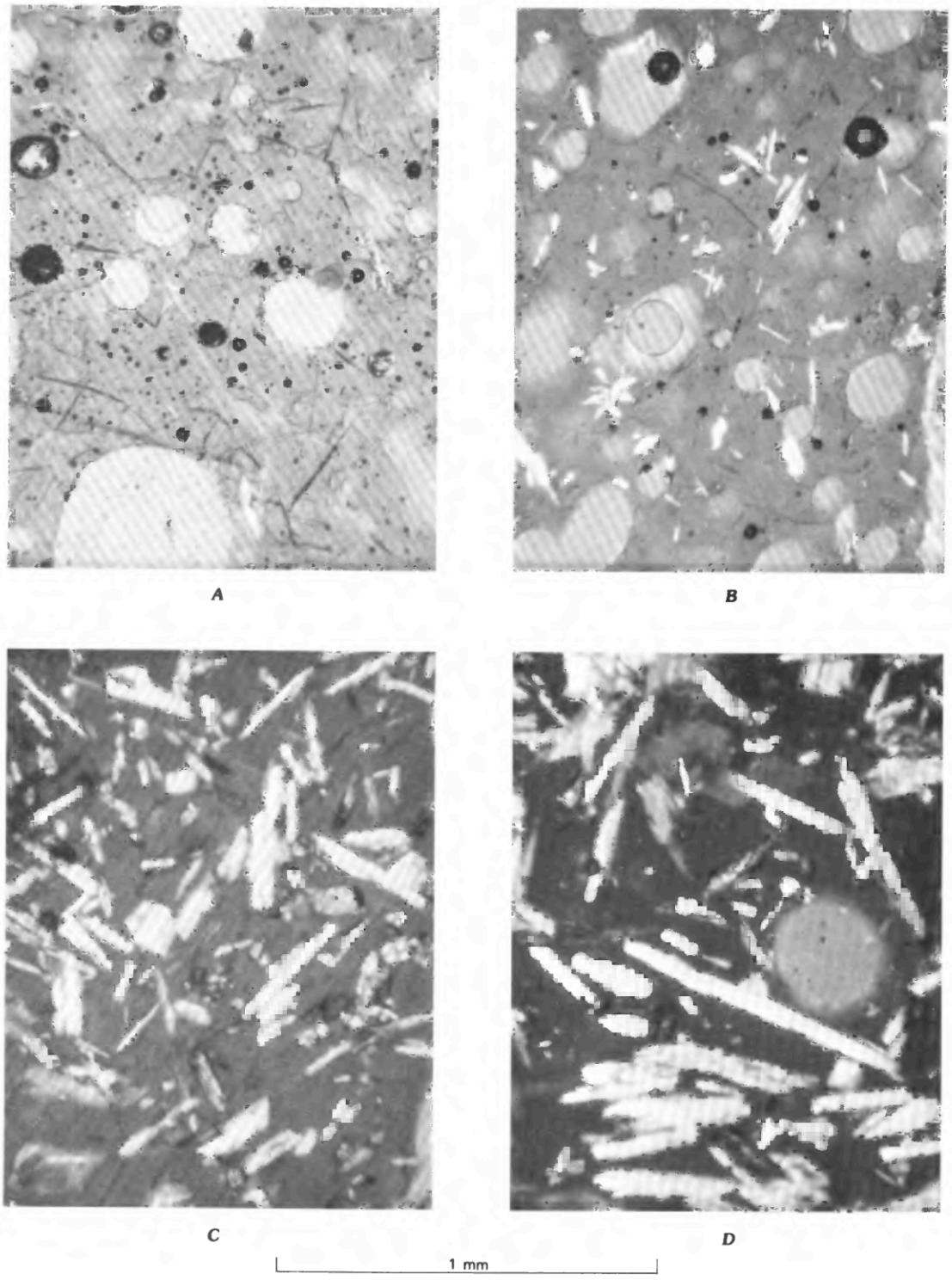

FIGURE 57.24.—Photomicrographs (plane light) of representative samples of 1984 Mauna Loa lava, showing progressive increase in size and abundance of microphenocrysts with time. Microphenocrysts are clear rectangles; circular features are gas bubbles (vesicles). ***A***, Sampled at about 0145 (H.s.t.) on March 25. Spatter from northeast side of 1949 cone, at 4,040 m. Sample MOK–1; 0.4 percent phenocrysts, 0.05 mm in average length. ***B***, Sampled at about 0515 on March 25. Spatter from upper northeast rift zone, at 3,650 m. Sample NER 5; 3.5 percent phenocrysts, 0.1 mm in average length. ***C***, Sampled at about 1750 on March 29. Pahoehoe from perched pond at 2,820 m. Sample NER 12/23; 21 percent phenocrysts, 0.3 mm in average length. ***D***, Sampled at about 0945 on April 14. Channel overflow near 2,870-m vent. Sample NER 12/66; 29.5 percent phenocrysts; 0.6 mm in average length.

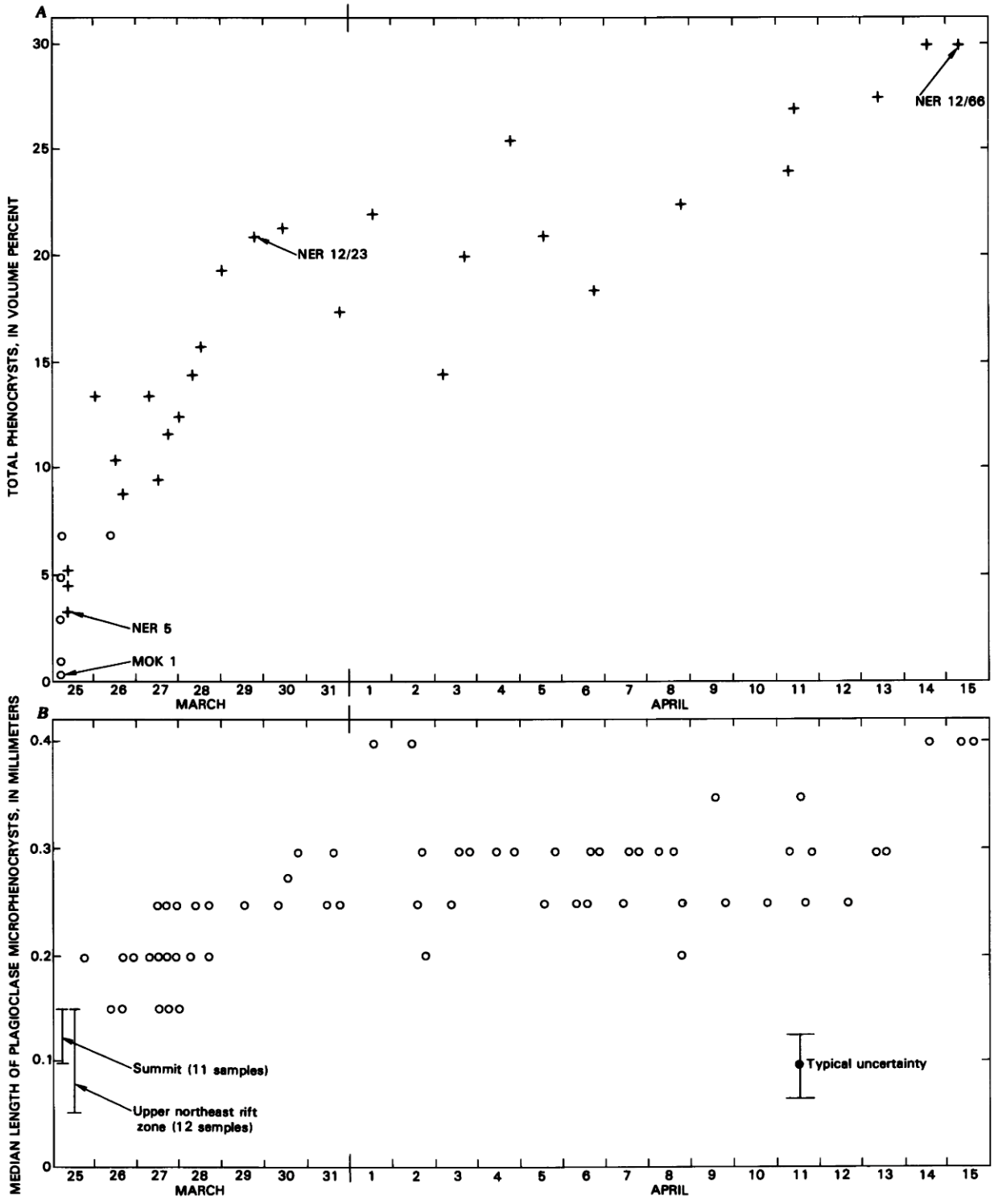

FIGURE 57.25.—Changes in abundance and size of microphenocrysts during 1984 eruption. Samples illustrated in figure 57.24 are identified. ***A***, Changes in abundance of microphenocrysts. Plus, data from petrographic point-counting of thin sections; dots, visual estimates of March 25–26 samples containing only sparse small microphenocrysts (less than 0.15 mm in average length). Values are believed accurate to within 10 percent; a major cause of uncertainty is in estimating areas of microphenocrysts smaller in diameter than the thickness of the thin section (0.03 mm). All samples are quenched glassy spatter or channel overflow. About one-half the originally collected samples of spatter were too vesicular to measure. ***B***, Changes in size of microphenocrysts. Median lengths of plagioclase microphenocrysts (about one-half the maximum length) were estimated visually from thin sections, by reference to a calibrated scale in the microscope ocular.

TABLE 57.2.—*Major-element composition of the 1984 Mauna Loa lava, from X-ray fluorescence analyses*

[Individual samples, selected to be representative, are described in table 57.1 and illustrated in figure 57.24. All values are in weight percent. Total iron listed as Fe_2O_3. Uncertainty of averages is plus or minus one standard deviation. Data provided by J.M. Rhodes; see Lipman and others, 1985]

Date	March 25		March 29	April 14	Entire eruption
Time	0145	0515	1750	0945	Average of 61 samples
Sample	MOK–1	NER–5	NER–12/23	NER–12/66	
SiO_2	51.51	51.56	51.71	51.27	51.54±.24
TiO_2	2.08	2.09	2.08	2.10	2.08±.02
Al_2O_3	13.75	13.69	13.69	13.60	13.65±.07
Fe_2O_3	12.08	12.11	12.17	12.08	12.07±.06
MnO	.17	.18	.17	.19	.18±.01
MgO	6.73	6.65	6.76	6.81	6.73±.08
CaO	10.57	10.55	10.57	10.43	10.50±.06
Na_2O	2.56	2.42	2.56	2.45	2.54±.11
K_2O	.385	.383	.391	.381	.385±.009
P_2O_5	.24	.25	.26	.24	.24±.01
TOTAL	100.13	99.87	100.38	99.55	99.92±.37

required, even if the pressure on upper parts of the rift conduit were atmospheric. Alternatively, the major loss of S, beginning at the summit reservoir, may have played a significant role in initiating crystallization. Unfortunately, few experimental data are currently available to permit evaluation of the role of small amounts of S on liquidus temperatures of basaltic magma.

RELATIONS OF CHANNEL VELOCITY, VOLUME, AND TIME

After the first three days of the eruption, as the vent geometry stabilized at the 2,900-m level and lava moved rapidly toward Hilo, we began establishing monitoring stations along the lava channel to permit repeated observations. At first, a primary need was to determine rates of lava movement downchannel for purposes of hazard evaluation; later, we focused more broadly on processes of channel evolution. For the first few days, limited helicopter support and poor weather confined observations to ground-accessible localities, and only a single observation point could be visited per day. Later in the eruption, working in two parties, we occupied as many as 4–6 stations per day. A total of 69 data sets are available for channel stations (table 57.3).

At each station, channel dimensions were determined, flow velocities measured, and morphologic observations made on the character of the flow, including photography. The resulting record of channel processes provides much of the basis for this paper. Complexities attendant to working on an erupting volcano caused some variations and problems in quality of the observations, as detailed in appendix 57.2. Total error in the channel-volume measurements, due mainly to uncertainties about channel depth, may be as large as 25 percent, but changes in channel volume at any station are believed accurate to about 10 percent, because the channel geometry tended to remain similar during the eruption or to deepen by measureable amounts through increase in levee height, especially for stations within the stabilized-channel zone.

Episodic short-term variations in channel volume, over periods of a few minutes to a few hours, were conspicuous in lower parts of the channel (transition zone), where surges could cause ephemeral channel-volume variations of as much as 50 percent; all plotted data are for observations made between obvious surges. Large short-term volume changes were also noted in stations near the vent, where fluctuations in fountain height related to varying gas release were associated with frequent changes in measured volume of 5–15 percent, occasionally as much as 40 percent. As noted earlier, some of these observed near-vent volume variations mainly reflect varying gas content and lava density, rather than true fluctuations in magma production rate (fig. 57.22). Several stations at mid-distance downchannel yielded volume variations of less than 5 percent when measured repeatedly over periods of several hours while larger fluctuations were being observed at the vent. Apparently, the short-term near-vent fluctuation tended to be smoothed out by downchannel flowage.

The most obvious feature of the channel data is a progressive decrease in channel discharge with lower elevation for any time during the eruption (fig. 57.26). In early April, discharges of 3.5×10^6–5×10^6 m^3/h were measured at the vent outlet, in comparision to discharges of only about 1.5×10^6 m^3/hr at 2,500-m elevation 5 km downchannel, and 0.5×10^6 m^3/hr at 1,900-m elevation 15 km from the vent. This decrease in discharge is interpreted as reflecting volume decrease of the lava due largely to volatile loss, because no overflows were occurring at this time along the intervening channel. The decrease in channel discharge downslope is paralleled by as much as a several-fold downslope increase in the density of quenched samples collected along the channel (fig. 57.20). These density changes alone can account for the changes in discharge, within sampling and measurement uncertainties.

A major feature of the eruption, documented from the channel stations, was a nearly constant rate of magma production during the middle part of the eruption, from March 31, when enough channel stations first became available, through April 6 (fig. 57.26). The steady state of activity during this interval is documented by 9 occupations of channel station 8 (1852 vent, 2,500-m elevation), which yielded channel discharges of $1.55\pm0.05\times10^6$ m^3/h, and by 10 occupations of several sites at station 4 (Upper Powerline area, 1,920–1,935 m), which yielded discharges in the range 0.40–0.55×10^6 m^3/h. Both these stations were within the stable-channel zone. The upper one (1852 vent) changed little during this time interval, except for partial crusting of the channel margins by pahoehoe scum (fig. 57.8*D*). Somewhat more variable discharges from the Upper Powerline sites are probably due to greater surge activity and levee building (figs. 57.9, 57.11*A*, 57.16*B*).

Before March 31, eruption rates at the 2,900-m vents had appeared roughly constant to observers, but several lines of evidence now demonstrate that eruption rates decreased during the first few days of the eruption. The first indication of such a decline came from early measurements of lava volumes reaching the channel stations at 1,800–1,900 m. Key evidence is from two channel stations established on March 28–29, which show higher discharges than observed at these elevations later during the eruption (fig. 57.26). The discharge measured for the 1,800-m station (Lower Powerline)

on March 28 is somewhat uncertain, because it depends on an aerial estimate of channel width under adverse weather conditions. Even if it is in error by one-third—the maximum that seems plausible—the resulting discharge (0.8×10^6 m^3/h) would still be twice that subsequently measured below 1,850 m.

No quantitative data are available for lava production at the vent before April 2, but repeated photography of the upper channel area document a major decline in channel flow levels between March 26 and 31 (fig. 57.27) that was not recognized by qualitative monitoring in the first few days of the eruption. Decreasing eruption rates early in the eruption are also indicated by analysis of lava areas and volumes, as discussed later.

In early April, the highest channel blockages and overflows were at about 1,850-m elevation (fig. 57.14), and the various Upper Powerline stations at 1,920–1,935 m show nearly constant volumes of flow. In contrast, the stations at 1,600–1,700 m show declines of about 50 percent in flow discharge between March 31 and April 4 (fig. 57.26), reflecting increasing loss of lava from the channel by blockages and overflows. By April 5, lava was no longer reaching any major channel below 1,850 m.

On April 6, a possible small decrease in discharge was measured at the 2,500-m station, which had yielded essentially constant results for the previous week, and by April 9 the channel was inactive to this level (fig. 57.26). This large change in channel discharge reflects the beginning of a further gradual decrease in eruptive rate at the main vent, from several million cubic meters per hour on April 6 to only a few hundred thousand cubic meters per hour by April 9 (fig. 57.28). Some of the decrease was taken up by new channels emanating from smaller uprift vents of the 2,900-m cluster, which robbed the main vent of part of its lava supply. Channels from the reopened uprift vents were north of flow 1 and initially carried as much as 0.5×10^6 m^3/h (density about 0.5 g/cm^3), about as much as flow 1.

Lava production continued to decline after April 9 and amounted to only about 0.1×10^6 m^3/h on April 13, the last full day of vent activity.

DISCUSSION

During the three-week eruption in 1984, the Mauna Loa aa flow and its distributary channel system underwent a complex morphologic evolution related to several intertwined changes in lava properties. These include decreases in eruptive volume; increased groundmass crystallization of the magma before venting; changes in effective viscosity and yield strength of the lava; degassing in the rift magma chamber, at the vent, and downchannel, which resulted in density increases of the lava; and probable physical maturation of the distributary channel itself. The dominant effects appear to have been (1) sympathetically increasing microphenocryst content, viscosity, and loss of gases from the pre-eruption magma reservoir and rift conduits; (2) constant lava composition and temperature; and (3) decreasing volume and average density of erupted material (fig. 57.29).

The eruption rate was nearly constant from March 30 to April 7 but declined drastically after April 7 (fig. 57.26). Major decreases also occurred early in the eruption, as indicated by (1) the high lava discharges measured at the two channel stations occupied on March 28–29, in comparison with results at similar elevations later during the eruption (fig 57.26); (2) the cessation of eruptive activity at the lower vents that fed flows 2–4 on March 25–27; and (3) interpreted rates of lava erupted per hour, based on the area covered as well as on the channel-station data (table 57.4).

Total volume of the erupted flows has been estimated at 220×10^6 m^3, based on mapped area of coverage and measured flow thickness (J.P. Lockwood, written commun., 1984). If the steady discharge rate determined from channel measurements between March 30 and April 6, about 0.4×10^6 m^3/h of relatively degassed channel lava at 1,900 m, is extrapolated back to initiation of the eruption, there is a shortfall of about 25 percent in volume (60×10^6 m^3). In contrast, the eruption rate for the early summit activity on March 25, as determined by area covered, was about 2.8×10^6 m^3/h, and rates for the first two days of activity from the 2,900-m vents were about 10^6 m^3/h (table 57.3). If the eruption rate further decreased from 10^6 m^3/h to 0.4×10^6–0.5×10^6 m^3/h during March 28–30, as indicated by the channel measurements (fig. 57.26), then the cumulative volume subsequently determined from the channel measurements (224×10^6 m^3, fig. 57.30) agrees reasonably well with the volume of 217×10^6 m^3 based on mapped area and flow thickness.

Decreases in eruption rate over time, which characterize many basaltic eruptions, have been inferred to relate to such factors as the release of elastic-strain energy from magma stored in the subvolcanic reservoir, availability of magma from depth during the eruption, and conduit evolution from dike to plug geometry (Wadge, 1981). An additional factor that appears to have been important in the 1984 Mauna Loa eruption, and perhaps for some others, is a change in magma rheology related to increasing crystal content of the erupted lava.

The increase in microphenocryst size and abundance (fig. 57.25) was roughly opposite to the decline in eruption rate (fig. 57.30). The resulting increase in magma viscosity (Shaw, 1969) was probably a major cause of termination of the eruption, as well as the pattern of uprift channel stagnation. At about 1,140 °C, the apparent viscosity of theoleiitic basalt containing an equilibrium crystal assemblage (about 25 volume percent) has been shown by field and laboratory measurements on Hawaiian basalt (Shaw, 1969, fig. 2; Shaw and others, 1968) to be approximately one order of magnitude greater than an undercooled Newtonian liquid lacking crystals. The changes in rheology, interpreted to have occurred largely in the pre-eruption magma chamber and rift conduits of Mauna Loa, are broadly similar to effects on the rheology of basaltic lava inferred to result from degassing during eruption and downslope flowage (Sparks and Pinkerton, 1978).

Such major decreases in eruptive rate in late March, if correctly interpreted, could explain the stagnation of flow 1 on March 30, but they do not account for the cessation of rapid advance and beginning of stagnation of flow 1*A* during the interval March 30–April 6. During this interval, both the eruption rate at the vent and transport in the channel system above about 1,850-m elevation remained constant, as indicated by the channel station data

TABLE 57.3.—*Dimensions and characteristics of lava channels and their changes with time, 1984 Mauna Loa eruption*

[Locations of channel stations on figure 57.1*B*. Distance, spacing of measuring points along channel bank. Depths estimated; see text for details. PWL, Peter W. Lipman; NGB, Norman G. Banks]

Measurement	Date (mo/d)	Hour (H.s.t.)	Condition	Distance (m)	Time (s)	Velocity (m/s)	Width (m)	Depth (m)	Flow rate (10^6 m^3/h)	Comments
Station 1: Lower channel 1A, elevation 1,600 m										
1	3/31	1130	stable	18	19	0.95	24	5	0.410	Conspicuous marginal shears, with velocities about 1 m/min, next to central well-defined channel. Channel velocities slow during surges which contain more viscous material. Maximum velocities occur just after surges. Gradient about 3°. Measured by PWL, NGB, and J. Fink.
2	3/31	1200	surge	18	22	.82	24	5	.355	
3	4/01	1200	--	18	28	.64	35	5	.405	Channel less defined than on 3/31, more choked with viscous debris. Although relatively steep gradient (about 5°) has migrated about 50 m downstream, adjacent to measurement site, velocities have still slowed. Because channel zone seems wider, flow rates have changed less than velocities. Measured by PWL and E. Wolfe.
4	4/01	1300	--	18	30	.60	35	5	.385	
5	4/02	1200	full	15	60	.25	40	6	.215	Channel less well defined than on 4/01, and choked with rubble; velocities much slowed. Measured by PWL, J. Fink, and H. Moore.
6	4/02	1230	low	15	110	.14	40	6	.120	
7	4/03	1520	slow	25	140	.18	52	5	.170	New station; old one unusable because of inboard levees. Top of active channel varies, 3 m below to 1 m above levees. Gradient 4.5°. Measured by NGB.
8	4/03	1550	normal	25	80	.31	52	5	.290	
9	4/03	1645	surge	25	90	.28	52	7	.364	
10	4/04	1350	--	25	163	.15	50	5	.138	Measured by NGB.
Station 2: Upper channel 1A, elevation 1,700 m										
11	4/03	1430	stable	15	45	.33	50	5	.295	Measured by PWL, J. Fink, and H. Moore.
12	4/03	1530	surge	15	30	.50	50	5	.450	
13	4/04	1345	stable	15	45	.3	25	5	.150	Sensitive to release of ponded lava at 1,800-m blockage. Surge provides upper limit in flow rate; estimates for stable periods likely to be more meaningful. Gradient about 4°. Measured by PWL, T. Neal, and H. Moore.
14	4/04	1430	stable	15	40	.4	25	5	.170	
15	4/04	1500	surge	15	25	.6	25	5	.270	
Station 3: Lower Powerline Road (flow 1, south side), elevation 1,800 m										
16	3/28	1310–1335		73	84	0.87	75	5	1.20	Depth fluctuations of as much as 2–3 m in 5 min, associated with surges; channel in two branches—only southern strand measured; channel broad, measured by visual aerial comparison with distance between power poles. Channel gradient about 2.5°. Measured by PWL and D. Clague.
17	3/28	1535–1605		73	80	.91	75	5	1.25	
Station 3: Lower Powerline Road (flow 1B), elevation 1,800 m										
18	4/06	1400	--	25	210	0.12	25	4	0.043	The channel flow slowed, and its upper surface subsided as we made these measurements. When checked an hour later, the head of flow 1B was captured by other overflows, and its channel was drained and empty. Gradient: 2.5°. Measured by PWL and T. Neal.
Station 4: Upper Powerline Road (site 1), elevation 1,900 m										
19	3/29	1300	blocks	30.2	25	1.20	13	6	0.335	Channel is within a gentle stretch related to large overflows and temporary ponding; probably deep as result. Higher velocities in center channel tend to push blocks to sides; more consistent measurements of maximum velocities obtained from small fragments in center channel. Channel gradient about 2.5°. Measured by PWL and E. Wolfe.
20	3/29	1400	fragments	30.2	18	2.75	13	6	.470	
21	3/31	1430	stable	30.2	23	1.3	13	6	.365	All measurements on small fast-moving fragments in center channel; lower level at 22 (about 1 m below levees) because of slightly higher gradient after drainage of ponded blockage downchannel. Gradient about 2.5°. Measured by PWL, NGB, and J. Fink.
22	3/31	1530	low	30.2	18	1.7	13	6	.470	
23	4/01	0830	stable	30.2	18	1.7	13	6	.470	Channel is sluggish and viscous; shear and pressure ridges are weakly developed on nearly stagnant channel sides. Measured by PWL and E. Wolf.
24	4/01	0930	blockage	30.2	19.5	1.6	13	6	.435	
25	4/02	1700	--	30.2	31	1.0	15	7	.370	Levees have increased in height about 2 m and largely obscure view of the channel: could only measure large boats during high stand of channel. Measured by PWL, J. Fink, and H. Moore.
26	4/03	1000	--	30.2	32.1	.94	18.3	7	.431	Levee height is 2.3 m above top of old ponded broad aa channel. Surge caused spreading of levee by 1 m in 15 min. Measured by NGB.
Station 4: Upper Powerline Road (site 2), elevation 1,930 m										
27	4/02	1600	--	20	9.5	2.1	14	4	0.455	New site, above upper cascade. Gradient about 3.5°. Measured by PWL, J. Fink, and H. Moore.
28	4/03	1320	--	20	12.6	1.6	14	5	.399	Measured by NGB.
Station 4: Upper Powerline Road (site 2A), elevation 1,930 m										
29	4/04	1200	--	23	12.3	1.9	15	5	0.500	Measured lava boats; low gradient due to blockages at head of middle cascade. Measured by PWL, T. Neal, and H. Moore.
Station 4: Upper Powerline Road (site 3), elevation 1,900 m										
30	4/04	1120	boats	20	7.5	2.7	15	4	0.580	Boats are sparse; channel level is 0.5–1 m below recent levee overflows. Gradient about 3°. Measured by PWL, T. Neal, and H. Moore.
31	4/04	1130	fragments	20	8.1	2.5	15	4	.530	
32	4/04	1140	fragments, surge	20	7.2	2.8	15	4	.600	
33	4/05	1100	--	20	9	2.2	20	4	.640	Little change since yesterday. Channel low and boats sparse, indicative of pond and surge forming upchannel. Measured by PWL and H. Moore.

TABLE 57.3.—*Dimensions and characteristics of lava channels and their changes with time, 1984 Mauna Loa eruption—Continued.*

Measurement	Date (mo/d)	Hour (H.s.t.)	Condition	Distance (m)	Time (s)	Velocity (m/s)	Width (m)	Depth (m)	Flow rate (10^6 m^3/h)	Comments
Station 4: Upper Powerline Road (site 4, flow 1B), elevation 1,900 m										
34	4/06	1100	--	24	14.9	1.6	30	3	0.520	New station, on uppermost gentle reach of flow 1B, just below breakout area. Channel here appeared broad and shallow, and its depth was confirmed later in day when the channel was drained and empty. Gradient 3°. Measured by PWL and T. Neal.
35	4/06	1130	--	24	14.9	1.6	30	3	.520	
Station 5: New south flow (flow 1C), elevation 1,950 m										
36	4/07	1000	--	15	10	1.5	10	5	270	Station is on channel carrying bulk of lava, just below currently most active ponding and breakout area at about 2,000 m. Gradient about 2.5°. Measured by PWL and H. Moore.
37	4/07	1545	--	15	16	1.1	10	5	.190	Many surges: difficult to make an average measurement, but clearly lower than this morning. Presumably, decrease reflects many overflow diversions. Measured by PWL and H. Moore.
Station 6: Main channel of flow 1, elevation 2,100 m										
38	4/07	1100	dropping	20	11	1.8	22	5	0.720	Stable channel, currently just above highest ponding area. Measured by PWL and H. Moore.
39	4/07	1120	after surge	20	10	2.0	22	5	.790	
Station 7: 1852 pahoehoe, elevation 2,300 m										
40	4/04	1630	--	20	4.7	4.23	15	5	1.15	Above highest area of blockages, levee building, and overflows. Gradient about 4.5°. Measured by PWL, T. Neal, and H. Moore.
41	4/08	1250	--	20	12.8	1.65	15	5	.424	Measured by NGB.
42	4/08	1310	--	20	6.5	3.1	15	5	.835	
Station 8: 1852 vent, elevation 2,500 m										
43	4/02	0900	site A	45	8.1	5.6	20	4	1.60	Measured velocities on small fragments in center channel. Gradient at site A is 6°; at site B, 4.5–5°. Measured by PWL, J. Buchanan-Banks, J. Fink, and H. Moore.
44	4/02	0930	site B	40	7.6	5.3	20	4	1.50	
45	4/03	0900	site A	45	8.7	5.2	20	4	1.50	No change evident. Measured by PWL, J. Fink, and H. Moore.
46	4/03	0920	site B	40	7.7	5.3	20	4	1.50	
47	4/03	1630	site B	40	7.5	5.3	20	4	1.54	No change since morning, despite reported 50 percent increase in production rate at vent. Measured by PWL and J. Fink.
48	4/04	0800	site B	40	7.5	5.3	20	4	1.55	No significant change. Measured by PWL, T. Neal, and J. Fink.
49	4/05	1415	site B	40	7.3	5.5	20	4	1.60	No change since previous day. Measured by PWL and H. Moore.
50	4/06	1100	site B	40	7.6	5.3	20	4	1.50	Surface channel actually only 10.3 m wide, because of crusting of margins. Measured by NGB.
51	4/06	1550	site B	40	7.6	5.3	20	4	1.50	No change, although level of channel at vent reported down 1 m. Measured by PWL and T. Neal.
52	4/07	1625	site B	40	7.5	5.3	18	4	1.40	Apparent slight decrease, from decreased estimated width of channel caused by crusting, but lava probably continues to flow slowly under crust. Measured by PWL and H. Moore.
53	4/08	0930	site B	40	14.2	2.8	9.2	4	.375	Surface is much grayer and has more scum than on 4/6. Volume is only about half as great. Gradient 3.5°. Measured by NGB.
Station 9: Middle channel, elevation 2,780 m										
54	4/09	1300	--	15	15	1.0	15	4	0.215	Broad shallow sheet-flow channel, the middle of three currently active around the west side of vent at 2,790 m (Puu 9,146). Measured by PWL and M. Rhodes.
Station 10: North channel, elevation 2,790 m										
55	4/09	1600	--	22	30	0.73	8	5	0.105	Narow channel, mostly well below levees. For visibility, had to measure during high channel flow. Measured by PWL and M. Rhodes.
56	4/10	1200	--	20	20	1	8	4	.100	Estimated velocity; channel on average 1–2 m lower than yesterday. Measured by PWL.
57	4/11	1215	--	15	10.1	1.5	12	3	.190	Measured by NGB.
58	4/12	1200	steady	16	25	.64	6	4	.055	Just upslope from station of previous day, which is now jammed by an overflow. Measured by PWL and R. Fodor.
59	4/12	1215	surge	16	14	1.1	6	5	.125	
Station 11: Vent outlet, elevation 2,850 m										
60	4/02	1130	--	30	1.7	17.8	21.5	3	4.50	Gradient is 6.5°; lava is fluffy; about 70 percent has bubbles. Measured by NGB.
61	4/04	1030	--	30	2.0	15	21	3	3.40	Flow rate is 1.5×10^6 m^3/h less than on 4/02. There is an antithetic relation between fountain height and channel level; at highest fountaining, channel flow rate is 5.2×10^6 m^3/h. Measured by NGB.
62	4/06	0900	--	30	2	15	20	3	3.5	Channel appears unchanged from 4/04; velocity estimated by NGB.
63	4/08	1145	--	30	4.65	6.45	21.5	3	1.50	Surface is grayer, but lava may be even fluffier than earlier. Flow rate half that of 2 days ago. Measured by NGB.
64	4/08	1600	--	20	10	2	30	3	.650	Channel much slower than in morning. Velocity estimated by NGB.
65	4/09	1040	--	40	17	2.4	5	3	.125	Channel contains viscous ropy pahoehoe. Measured by PWL and M. Rhodes.
66	4/09	1130	higher	40	12.5	3.2	5	4	.230	
Station 12: West vent, elevation 2,900 m										
67	4/08	1620	--	--	--	2	30	2	0.430	Velocity estimated by NGB.
68	4/12	1400	--	20	10.5	1.9	5	5	.170	Station is about 100 m downchannel from active vents. Lava is fluffy, like cotton candy. Degassed flow rate probably about 30×10^3–40×10^3 m^3/h. Gradient about 3°. Measured by PWL and J. Lockwood.
69	4/13	1400	--	20	16	1.25	5	5	.110	Channel flow is steeper but slower than yesterday, even though measured at high fountain level. Gradient 4.5°. Measured by PWL and NGB.

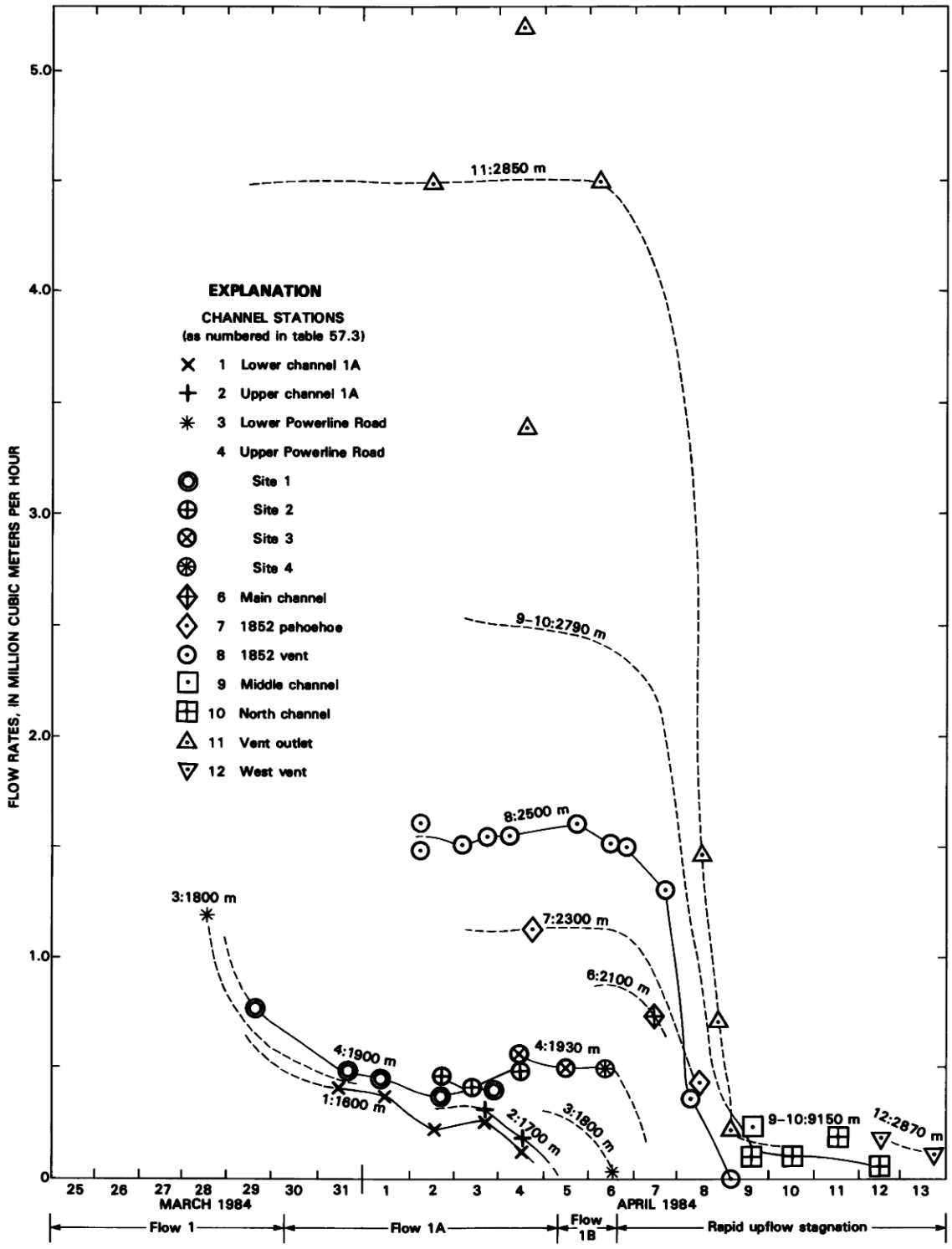

FIGURE 57.26.—Changes in channel discharge with time, 1984 Mauna Loa eruption as measured at channel stations (identified by number; see table 57.3). Solid lines connect repeated observations at individual sites; dashed lines are interpreted trends for discharges based on data at other stations and qualitative observations of channel evolution.

(fig. 57.26). Additional factors came into play during this time interval to cause stagnation of the flow and channel system, and these factors may also have had a role in the early stagnation of flow 1 before March 30.

Lava temperatures at the vent remained nearly constant throughout the eruption, as did temperatures of the most fluid parts of the downchannel flows (fig. 57.19). The latter is thought to have resulted from the heat of microlite crystallization and from thermal feedback associated with deformation of the silicate melt fraction during downchannel flow. Despite the uniform eruptive temperature and chemical composition, the proportion of solid and pasty material (reflecting greater groundmass crystallization) gradually increased in lower reaches of the channel system, raising both the bulk viscosity and the yield strength of the lava. Even in the zones of stabilized and transitional flow, increased downflow sluggishness in the channel indicated progressive increase in viscosity of the fluid matrix between the solid and pasty material. These downchannel effects must have been caused by changes in some intrinsic property of the lava other than decreasing temperature. Decreased gas content and increased groundmass microlite crystalization seem the most likely candidates, as discussed earlier in this paper and as previously suggested for basaltic flows in general by Sparks and Pinkerton (1978).

We infer that decreased gas content played a large role, because fluidity of the flow appears to be at least in part related to the ease of deformation of the silicate liquid that constitutes the vesicle walls. The 80–90 percent decrease in vesicularity of lava in the channel from the vent to the zone of dispersed flow and the accompanying proportional increase in vesicle wall thickness of the silicate melt may have increased the bulk viscosity by several hundred percent.

The greater numbers of microlites downflow must also have increased the effective viscosity of the channel fill, much in the manner that the increased microphenocryst population in the erupted lava raised the viscosity of the lava at the vent. Degassing and crystallization influenced the viscosity and thus the behavior of the lava in differing ways. Degassing of the lava flexed the silicate liquid to produce thermal feedback, adiabatically cooled the lava, and increased the proportion of viscous silicate liquid present. Crystallization heated the lava but also increased its bulk viscosity. The combination of these effects apparently reduced the rate of flow at the vent, delayed temperature decreases downflow and probably also in the lava conduit, produced the conditions required for the pahoehoe-aa transition, and ultimately contributed to the maturation and stagnation of flows during the Mauna Loa eruption.

A further process possibly contributing to stagnation of the flow system was maturation of the channel structures with time. Solidification and increasingly brittle behavior of the channel banks, deepening of the channels by levee growth and possibly by erosion of the channel floor, and crusting over of channel margins and eddies are among the unidirectional processes that could have helped destabilize the channel system during the course of the eruption, regardless of changes at the vent. Such maturation processes could have caused greater formation of channel debris, initially triggered by small fluctuations in vent eruption rate, that led to increasingly larger debris blockages, overflows, and surges downchannel.

Deviations from simple correlations between length of lava flows and eruption rate (Walker, 1973), which have been demonstrated for Hawaiian flows (Malin, 1980), may largely result from the superimposed effects of variable vesiculation, density, undercooling, and crystallinity of the lava. Increased undercooling and crystallinity, decreased vesicularity, and associated increased density would all promote higher effective bulk viscosity and yield strength in basaltic flows, causing transitions from pahoehoe to aa and reducing the length of flows at any constant eruption rate. In contrast, long-lived eruption at liquidus temperature would promote transportation of pahoehoe in lava tubes, permitting lava flows to travel farther. The rheology of lava erupted as gas-rich foam (reticulite, in the case of Hawaiian basalt) that deflates during emplacement will be markedly different from that of degassed lava; such contrasts may extend to highly silicic compositions (Eichelberger and Westrich, 1984). Proposed simple correlations of viscosity and yield strength of lavas with chemical parameters such as silica content (Hulme, 1974) are also imperfect (Moore and others, 1978), perhaps in large part because of the complicating factors just listed.

Finally, it should be noted that the evolution of the 1984 flow system was similar in volume, duration, and eruptive style to several previous historical (since the mid-19th century) rift eruptions of Mauna Loa. Field and photogeologic examination indicates that patterns of upslope stagnation of the distributary channel system characterized many of these earlier events, including the 1852 and 1942 flows that are adjacent to the 1984 flows. Sparse petrographic data indicate that other major historical rift flows (1843, 1926, 1935, 1942, 1950; northeast rift samples collected by J.P. Lockwood and G. Lockwood) also show trends of increasing content of microphenocrysts during the eruption. Similar observations for prolonged summit eruptions, such as those of 1940 or 1949, would be particularly significant because they could permit distinction between the effects of depressurization of the summit reservoir and degassing along the rift conduits. Additional studies of the relations between eruption style, flow evolution, and lava crystallinity of earlier Mauna Loa eruptions are in progress.

More extensive observations are needed on the interrelations between gas content, crystallinity, eruption temperature, and viscosity of erupting basaltic lava. Changes in lava discharge rate, temperature, density, bulk chemistry, and abundance of microphenocrysts were key determinable parameters for the 1984 eruption that should be monitored closely in future activity. Such studies may answer some remaining questions: does lava temperature commonly remain constant during long-lived eruptions, even during periods of declining discharge? Does density of spatter typically decrease during an eruption? Does the development of lava tubes and long-traveled pahoehoe during prolonged eruptions require eruption temperatures near the one-atmosphere liquidus, or at least retardation of major degassing and attendant undercooling before eruption? If eruptions of undercooled lava, marked by increasing microphenocryst populations, can be shown to generate aa flows close to the vent, observations of lava temperature and crystallinity can have important implications for assessing volcanic hazards during early phases of major basaltic eruptions.

A

B

FIGURE 57.27.—Upper channel system of flow 1, as viewed from vent at 2,790 m (Puu 9,146 ft), approximately 4 km from the active vent at 2,900-m elevation. ***A***, At 0900 on March 26. Channel banks of flow 1 are full or overflowing; small bright specks to right of active channel are areas of still-glowing lava that indicate a large overflow within the previous hour. Small channel of flow 2, fed by low fountains, is visible at upper left. Discharge (normalized to density 2.0 g/cm^3) estimated at 1.0×10^6–1.5×10^6 m^3/h. ***B***, At 1600 on March 31. Lava confined completely within channel banks; several forks of the channel and intervening islands have emerged. Despite lower channel level, compared to 5 days earlier, fountain height is higher, probably reflecting a higher proportion of exsolved gases. Discharge (normalized to density 2.0 g/cm^3) estimated at 0.5×10^6–0.6×10^6 m^3/h. Prominent spatter ramparts in left distance mark vents for flows 2–4; these grew rapidly early in the eruption but were inactive after March 27.

A

B

FIGURE 57.28.—Changes in fountain height and lava production, as seen from vent outlet (channel station 11) during 1984 Mauna Loa eruption. ***A***, April 2: Vent fountains about 40 m high, well above the spatter rampart. Fluffy channel lava was moving at about 60 km/h, with a discharge rate of about 4.5×10^6 m^3/h (table 57.3, no. 60). In contrast to the lower portions of the stable-channel zone (see figs. 57.8C, 57.10), a broad central part of the channel is moving with plug flow. Velocity gradients are confined to within a few meters of the channel bank. ***B***, April 8, at 1145 h: Vent fountains only 5–10 m high, no longer visible above the spatter rampart. Velocity of the channel lava has declined to about 23 km/h, and the discharge rate is about 1.5×10^6 m^3/h (table 57.3, no. 63); later in the afternoon of April 8, discharge declined by an additional 50 percent. Nevertheless, the level of lava in the channel remains nearly as high as when the eruption rate was several times greater. Note that the highest part of the channel levee visible on April 2 has caved into the channel, presumably to form lava boats.

TABLE 57.4.—*Estimated daily lava production rates and cumulative volumes, 1984 Mauna Loa eruption*

Date (mo/d)	Rate (10^6 m³/h)	volume (10^6 m³)	Cumulative volume (10^6 m³)	Note
3/25	2.8×6 h	25×2/3	16.7	1
3/25	.7×8 h	5.8	22.5	1
3/25	1.1×8 h	8.9	31.4	2
3/26	1.1	26.1	57.5	2
3/27	1.1	26.1	83.6	2
3/28	1.1–1.2	26.1	109.7	3
3/29	.75	18.0	127.7	4
3/30	.5	12.0	139.7	3
3/31	.4	9.6	149.3	3
4/1	.4	9.6	158.9	3
4/2	.4	9.6	168.5	3
4/3	.4	9.6	178.1	3
4/4	.4	9.6	187.7	3
4/5	.4	9.6	197.3	3
4/6	.4	9.6	206.9	3
4/7	.3 (1.2)	7.2	214.1	5
4/8	.16 (.65)	3.6	217.7	5
4/9	.10 (.40)	2.4	220.1	5
4/10	.07 (.28)	1.7	221.8	5
4/11	.05 (.20)	1.2	223.0	5
4/12	.04 (.17)	.7	223.7	5
4/13	.02 (.08)	.5	224.2	5
4/14	.00	.0	224.2	6

1. Hourly production rates for early eruptions from summit (0130–0730, 3/25) and upper rift zone (0900–1700, 3/25) determined by area and thickness measurements (J.P. Lockwood, written commun., 1984). Summit lava is mostly shelly pahoehoe (estimated average density, 1.5 g/cm³), so volume is reduced by a third to make comparable to volume estimates for later eruptive phases (estimated average density, 2.0 g/cm³).
2. Hourly production rate for first 48 h of eruption from 2,900-m vent area (1600 3/25 to 1600 3/27), determined by area and thickness estimates, based on field observations by the authors. Data permit a decay in eruption rate, as alternative to constant rate, during this interval.
3. Production rate determined from channel measurements at 1,800 to 1,900-m stations (table 57.3). Estimated average density, 2.0 g/cm³.
4. Production rate interpolated between rates for previous and subsequent days.
5. Production rate determined from channel measurements at 2,500 to 2,850-m stations (table 57.3). Estimated average density, 0.5 g/cm³; accordingly, observed discharges (in parentheses) are reduced by three-quarters to make comparable to other measurements.
6. End of eruption.

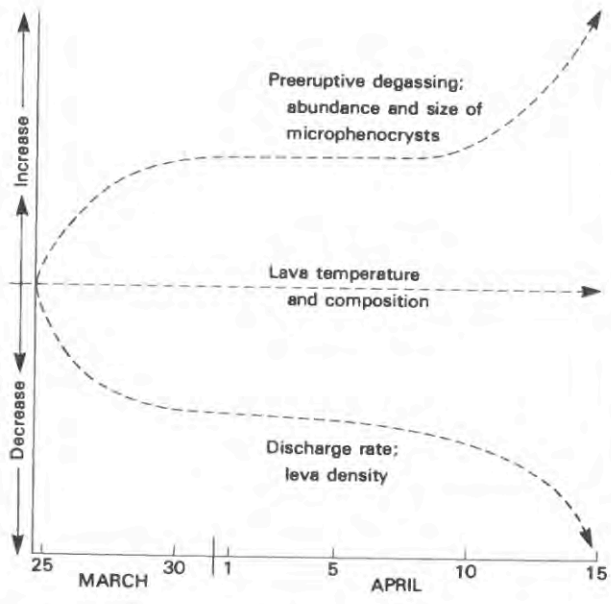

FIGURE 57.29.—Diagram illustrating interdependent time relations between eruptive volume, microphenocryst content, lava composition, eruption temperature, amount of degassing, and lava density during 1984 Mauna Loa eruption.

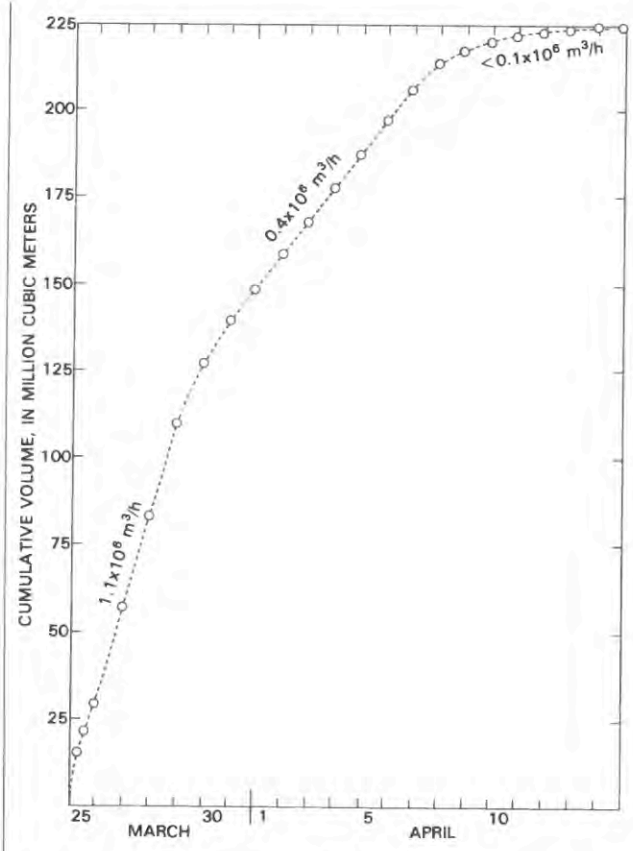

FIGURE 57.30.—Interpreted cumulative volume of erupted lava in 1984 Mauna Loa eruption plotted against time. Data from table 57.4.

REFERENCES

Alt, W.U., Eaton, J.P., and Richter, D.H., 1961, Lava temperatures in the 1959 Kilauea eruption and cooling lake: Geological Society of America Bulletin, v. 72, p. 791–794.

Banks, N.G., and Hoblitt, R.P., 1981, Summary of temperature studies of 1980 deposits, *in* Lipman, P.W., and Mullineaux, D.R., eds., The 1980 eruptions of Mount St. Helens, Washington: U.S. Geological Survey Professional Paper 1250, p. 295–313.

Borgia, A., Linneman, S., Spenser, D., Morales, L.D., and Andre, J.B., 1983, Dynamics of lava flow fronts, Arenal Volcano, Costa Rica: Journal of Volcanology and Geothermal Research, v. 19, p. 303–330.

Casadevall, T., Krueger, A., and Stokes, B., 1984, The volcanic plume from the 1984 eruption of Mauna Loa, Hawaii [abs.]: Eos, Transactions of the American Geophysical Union, v. 65, p. 1133.

Cigolini, C., Borgia, A., and Casertano, L., 1984, Intra-crater activity, aa-block lava, and flow dynamics, Arenal Volcano, Costa Rica: Journal of Volcanology and Geothermal Research, v. 20, p. 155–176.

Decker, R.W., Koyanagi, R.Y., Dvorak, J.J., Lockwood, J.P., Okamura, A.T., Yamashita, K.M., and Tanigawa, W.R., 1983, Seismicity and surface deformation of Mauna Loa Volcano, Hawaii: Eos, v. 64, p. 545–547.

Eichelberger, J.C., and Westrich, H.R., 1984, Degassing of magma in an obsidian flow and inferred degassing behavior at depth, *in* Active tectonic and magmatic process beneath Long Valley caldera, eastern California: U.S. Geological Survey Open-File Report 84–939, p. 147–150.

Finch, R.H., and Macdonald, G.A., 1953, Hawaiian volcanoes during 1950: U.S. Geological Survey Bulletin 996–B, 89 p.

Garcia, M.O, Byers, C.D., Wolfe, E.W., and Rhodes, J.M., 1984, Chemistry and mineralogy of lavas from the continuing eruption of Kilauea Volcano, Hawaii [abs.]: Eos, v. 65, p. 1130.

Greenland, L.P., Okamura, A., and Stokes, J.B., in press, Constraints on the mechanics of eruption of Puu Oo, *in* Wolfe, E.W., ed., The Puu Oo eruption of Kilauea Volcano, Hawaii: the first 1-1/2 years: U.S. Geological Survery Professional Paper.

Greenland, L.P., Rose, W.I., and Stokes, J.B., 1985, An estimate of gas emissions and magmatic gas content from Kilauea Volcano: Geochemica et Cosmochimica Acta, v. 49, p. 125–129.

Haggarty, S.E., 1981, Volatiles in planetary basalts: hydrogen, carbon, and sulfur gas species, *in* Basaltic volcanism on the terrestrial planets: New York, Pergamon Press, Basaltic Volcanism Study Project, p. 385–398.

Hulme, G., 1974, The interpretation of lava flow morphology: Geophysical Journal of the Royal Astronomical Society, v. 39, p. 361–383.

Jones, D.L., Silberling, N.J., Gilbert, W., and Coney, P., 1982, Character, distribution, and tectonic significance of accretionary terranes in the Central Alaska Range: Journal of Geophysical Research, v. 87, p. 3709–3717.

Kirkpatrick, R.J., 1976, Toward a kinetic model for the crystallization of magma bodies: Journal of Geophysical Research, v. 81, p. 2565–2571.

——— 1977, Nucleation and growth of plagioclase in the Hawaiian lava lakes Makaopuhi and Alae: Geological Society of America Bulletin, v. 88, p. 78–84.

Lipman, P.W., Banks, N.G., and Rhodes, J.M., 1985, Gas-release induced crystallization of 1984 Mauna Loa magma, Hawaii, and effects on lava rheology: Nature, v. 317, p. 604–607.

Lockwood, J.P., Banks, N.G., English, T.T., Greenland, L.P., Jackson, D.B., Johnson, D.J., Koyanagi, R.Y., McKee, K.A., Okamura, A.T., and Rhodes, J.M., 1985, The 1984 eruption of Mauna Loa Volcano, Hawaii: Eos, v. 65, p. 169–171.

Lockwood, J.P., Koyanagi, R.Y., Tilling, R.I., Holcomb, R.T., and Peterson, D.W., 1976, Mauna Loa threatening: Geotimes, v. 21, p. 12–15.

Lofgren, G.E., 1981, Comparative petrography and cooling rates, *in* Basaltic volcanism on the terrestrial planets: New York, Pergamon Press, Basaltic Volcanism Study Project, p. 364–370.

Macdonald, G.A., 1953, Pahoehoe, aa, and block lava: American Journal of Science, v. 251, p. 169–191.

——— 1972, Volcanoes, Englewood Cliffs, New Jersey, Prentice Hall Inc., 510 p.

Macdonald, G.A., and Abbott, A.T., 1970, Volcanoes in the Sea: Honolulu, University of Hawaii Press, 441 p.

Malin, M.C., 1980, Lengths of Hawaiian lava flows: Geology, v. 8, p. 306–308.

Moore, H.J., Arthur, D.W.G., and Schaber, G.G., 1978, An estimate of the yield strength of flows on the Earth, Mars, and Moon: Lunar and Planetary Science Conference, 9th, Proceedings, p. 3351–3378.

Moore, J.G., 1965, Petrology of deep-sea basalt near Hawaii: American Journal of Science, v. 263, p. 40–52.

Moore, R.B., Dzurisin, D., Eaton, G.P., Koyanagi, R.Y., Lipman, P.W., and Lockwood, J.P., 1980, Preliminary report on the 1977 eruption of Kilauea Volcano, Hawaii: Journal of Volcanology and Geothermal Research, v. 7, p. 189–210.

Murase, T., 1962, Viscosity and related properties of volcanic rocks at 800° to 1400°C.: Hokkaido University, Journal of the Faculty of Science, Ser. 7, v. 1, p. 487–584.

Neal, C.A., Duggan, T.A., Wolfe, E.W., and Brandt, T.L., in press, Lava samples, temperatures and compositions; Puu Oo eruption of Kilauea Volcano, Hawaii, phases 1–20, *in* Wolfe, E.W., The Puu Oo eruption of Kilauea Volcano, Hawaii: the first 1-1/2 years: U.S. Geological Survey Professional Paper.

Nielsen, R.L., and Dungan, M.A., 1983, Low pressure mineral-melt equilibria in natural anhydrous mafic systems: Contributions to Mineralogy and Petrology, v. 84, p. 310–326.

Peterson, D.W., and Tilling, R.I., 1980, Transition of basaltic lava from pahoehoe to aa, Kilauea Volcano Hawaii: field observations and key factors: Journal of Volcanology and Geothermal Research, v. 7, p. 271–293.

Rhodes, J.M., 1983, Homogeneity of lava flows: chemical data for historic Mauna Loa eruptions: Journal of Geophysical Research, v. 88 (supplement), p. A869–A879.

Shaw, H.R., 1969, Rheology of basalt in the melting range: Journal of Petrology, v. 10, p. 510–535.

Shaw, H.R., Wright, T.L., Peck, D.L., and Okamura, R., 1968, The viscosity of basaltic magma: an analysis of field measurements in Makaopuhi lava lake, Hawaii: American Journal of Science, v. 266, p. 225–264.

Sparks, R.S.J., and Pinkerton, H., 1978, The effect of degassing on the rheology of basaltic lava: Nature, v. 276, p. 385–386.

Sparks, R.S.J., Pinkerton, H., and Hulme, G., 1976, Classification and formation of lava levees on Mount Etna, Sicily: Geology, v. 4, p. 269–271.

Swanson, D.A., 1973, Pahoehoe flows from the 1969–1971 Mauna Ulu eruption, Kilauea Volcano, Hawaii: Geological Society of America Bulletin, v. 84, p. 615–626.

Swanson, D.A., Duffield, W.A., Jackson, D.B., and Peterson, D.W., 1979, Chronological narrative of the 1969–71 Mauna Ulu eruption of Kilauea Volcano, Hawaii: U.S. Geological Survey Professional Paper 1056, 55 p.

Ulrich, G.E., Wolfe, E.W., Hoffman, J.P., and Neal, C.A., 1984, Continuing eruption of east rift zone, Kilauea Volcano, Hawaii [abs.]: Eos, v. 65, p. 1130.

Wadge, G., 1978, Effusion rate and the shape of aa lava flow-fields on Mount Etna: Geology, v. 6, p. 503–506.

——— 1981, The variations of magma discharge during basaltic eruptions: Journal of Volcanology and Geothermal Research, v. 11, p. 139–168.

Walker, D.R., Kirkpatrick, R.J., Longhi, J., and Hays, J.F., 1976, Crystallization history and origin of lunar picritic basalt 12002: phase equilibrium, cooling rate studies, and physical properties of the parent magma: Geological Society of America Bulletin, v. 87, p. 646–656.

Walker, G.P.L., 1973, Length of lava flows: Philosophical Transactions of the Royal Society of London, v. A274, p. 107–118.

Wentworth, C.K., and Macdonald, G.A., 1953, Structures and forms of basaltic rocks in Hawaii: U.S. Geological Survey Bulletin 994, 98 p.

Wright, T.L., and Fiske, R.S., 1971, Origin of the differentiated and hybrid lavas of Kilauea Volcano, Hawaii: Journal of Petrology, v. 12, p. 1–65.

Wright, T.L., Kinoshita, W.T., and Peck, D.L., 1968, March 1965 eruption of Kilauea Volcano and the formation of Makaopuhi lava lake: Journal of Geophysical Research, v. 73, p. 3181–3205.

Yoder, H.S., and Tilley, C.E., 1962, Origin of basalt magmas: an experimental approach: Journal of Petrology, v. 3, p. 342–532.

APPENDIX 57.1

LAVA-TEMPERATURE AND DENSITY MEASUREMENTS

The temperatures in table 57.1 were measured by direct insertion of thermocouples into lava (code T, table 57.1) and by two-color infrared pyrometer readings of fountains or noncrusted fast-flowing lava (code H). Similar equipment has been used to measure temperatures of varied volcanic products (Banks and Hoblitt, 1981; Neal and others, in press). Samples for density and other petrologic studies were collected at many of the sites where temperatures were measured.

THERMOCOUPLE EQUIPMENT

Several configurations of commercial thermocouples were used, in which chromel-alumel wires imbedded in MgO were sheathed with and grounded to Inconel high-temperature stainless steel. Grounded thermocouples, which respond 3–5 times faster than ungrounded versions, have proved to be durable and resistant to thermal and mechanical fatigue as well as corrosion under difficult field conditions.

For slow-moving pahoehoe, small-gauge thermocouples (1.5-mm sheath diameter, 3–10 m long; code 1 in table 57.1) were preferred because of their small thermal mass. Temperatures obtained with such thermocouples were within 5–10 °C of equilibrium with the melt in 1–2 minutes and completed equilibration within the next 2–3 minutes. Where rigidity was required to insert the thermocouple into lava, the thermocouple was wound around a light steel rod, so that the thermocouple tip extended 20–30 cm beyond the rod.

For moving pahoehoe or dense aa, the small-gauge wire usually proved too flexible to insert, and heavier-gauge thermocouples were required. For these situations, 6-mm-diameter Inconel-sheathed thermocouples (code 2, table 57.1) provided excellent results. Response times with the heavy-gauge wire were longer, taking 3–5 minutes to approach within 5 °C of the melt temperature and up to 10 minutes for full equilibration.

Thermal and mechanical stress often caused failure of the thermocouple tips after several insertions, particularly for the small-gauge type. When this happened, 3–6 cm of the faulty end were cut off, and the thermocouple wires were exposed with wire strippers and twisted together. The repaired thermocouple could then be immersed directly in melt to obtain additional temperatures. The double advantage of the exposed tip was an extended life for the thermocouple and a response time about 5 times faster. Calibration of sheathed and bare thermocouple wires in the field and in a test kiln indicated no systematic differences. Code B in table 57.1 indicates that the thermocouple tip was directly exposed to the lava; code C measurements were with a fully clad and grounded thermocouple tip.

Thermocouple voltages were converted to temperatures using direct reading digital voltmeters that were compensated electronically (cold junction). Five meters from two manufacturers were used. The meters were periodically checked against precise millivolt calibrators, which themselves were periodically tested against a laboratory millivolt meter. The meters consistently agreed within ±1 °C of the temperature indicated by the calibrators, as did temperatures obtained by two or more meters sequentially attached to a single thermocouple which had been implanted and equilibrated in lava or a test kiln (see also Banks and Hoblitt, 1981). An exception was a meter, which previously gave good numbers, that was exposed inadvertantly to intense radiation during a measurement; this meter read +4 °C high when next calibrated, and data gathered in the interim were accordingly corrected.

FIELD TECHNIQUES

Observers and thermocouple meters were shielded from the intense radiative heat of the lava by use of a commercial aluminized heat suit (fig. 57.6*B*) or a sheet of aluminum roofing that was fitted with a handle to avoid contact with the metal. Although both shielding techniques were at times used simultaneously, the sheeting was preferred because of increased body ventilation, mobility, and superior visibility and hearing afforded the observers. At an open lava channel or aa front, the heat suit was frequently the only adequate protection.

Techniques in pahoehoe melts were similar in most situations. After preheating the small-gauge thermocouple tip to 700–900 °C for several seconds, it was inserted slowly to a depth of 10–20 cm in an area of melt where no crust had formed. Undesirable growth of a lava icicle or sheath, particularly a problem with the large-gauge thermocouple, could be minimized by working the tip back and forth during slow insertion.

Generally, two people worked together: one person would immerse and maneuver the thermocouple, attempting to avoid hitting any developing crust that might damage or break the wire, and the other would watch for approaching lava, read the meter, and frequently hold the protective shield. Temperatures were read aloud, and as equilibrium was approached and the thermocouple stabilized, a single reading was recorded.

Most temperatures of aa flows were measured with the 6-mm-diameter thermocouples because of their superior rigidity and resistance to breakage. The probe was clamped to an iron rod 4–6 m long, with 20–30 cm extending beyond the rod, preheated to lessen the thermal shock, and pushed into a brightly incandescent part of an advancing flow front. Depending on the viscosity of the melt and the thickness of the chilled aa rind, the probe might readily penetrate the fluid core of the flow. At times, the observer had to lean full weight against the rod in order to force penetration. In most cases, the probe was gradually enveloped by the advancing flow to depths of 2–6 meters. Acceptable penetration and a stable temperature reading generally took 15–30 minutes, and most probes were not recovered. Temperatures were monitored at a safe distance from the rolling incandescent boulders typical of advancing aa fronts, by using an extension cord to the meter.

THE TWO-COLOR INFRARED PYROMETER

Temperatures of the fountains and fast-flowing, uncrusted lava near the vent were measured by a hand-held two-color, infrared pyrometer (HOTSHOT). The two colors allow instant direct calculation of emissivities, thereby yielding relatively accurate temperatures for the radiating body. The instrument has interchangeable lenses, and to narrow the field of view, we used a telephoto lens and an almost-closed aperature. This gave a field of view only a few centimeters across at 5 m and less than 1 m^2 at 30 m distance. The subject and the light-emitting diode display are viewed simultaneously through the eyepiece, and the instrument has an internal reference calibrator, used to adjust for drift before and after each shot.

The HOTSHOT produced stable fountain temperatures that were similar or slightly above the best thermocouple measurements in near-vent flows. Several precautions were required to obtain accurate temperatures: (1) the instrument was immobilized through ground-bracing or use of a tripod; (2) the area viewed was kept small, to eliminate inclusion of sky or crusted spatter falling in front of the active fountains; (3) little or no cooling lava could be between the subject and the instrument; and (4) measurements were avoided over distances greater than 30–40 m. Item (1) is necessary to minimize fluctuations in the readings. Item (2) is to prevent the two detectors from reading separate subjects, which causes calculation of erroneously high or low emissivities. Items (3) and (4) are precautions because certain gasses, probably water vapor, cause different absorption of the two infrared wavelengths. Empirically, we found that unrealistically high numbers result from long shots or shots over degassing lava.

CLASSIFICATION OF THE DATA

Several criteria were used to classify the quality of thermocouple and HOTSHOT temperature data (table 57.1). Code I (icicle) indicates that the thermocouple tip acquired an insulating sheath of lava before stabilizing at the actual lava temperature. These measurements were marked by unstable temperatures that peaked 10–100 °C below other temperatures at the same or a similar locality, and by the icicle growth on the thermocouple when withdrawn. Code F (failed) indicates that the thermocouple tip failed at the indicated temperature without stabilizing, or that penetration into the melt was poor. Code P (poor) indicates that nonideal atmospheric conditions or fluctuating values occurred during a HOTSHOT measurement. Code E (equilibrium) indicates that a stable temperature in equilibrium with the lava was obtained, but that geologic conditions suggested that the lava had cooled relative to temperatures at the vent or main channel. Spatter-fed flows, thin rapidly cooling overflows from lava rivers, and lava held in prolonged storage in lava tubes consistently produced temperatures 5–10 °C below those obtained in obviously superior geological settings. Code G (good) indicates measurements that we consider superior by virtue of

temperature stablility, condition of the probe or path of sight, and quality of the geologic location. Confidence in the G-coded measurements grew as identical temperatures within ±3 °C were obtained at the same locations day after day, both at the vents and down the main channel.

G-coded thermocouple measurements were made either in slow-moving pahoehoe that was insulated from the atmosphere or in aa where the probe tip penetrated into the fluid core and remained stable for 5–20 minutes. Ideal situations were pahoehoe toes fed by lava tubes that tunneled directly through the spatter rampart. The best situations for determining downflow lava temperatures were active pahoehoe fronts or margins, oozes through cracks in accretionary levees at the edges of the main channel, lava tubes fed by and near the channel, thick aa overflows near the channel, and the fluid cores of aa fronts.

SAMPLING AND DENSITY DETERMINATIONS

Several types of samples were collected to study changes in chemistry, mineralogy, texture, and density of the melt during the eruption. Many samples were collected concurrently with temperature measurements. Samples from the channels, channel overflows, and pahoehoe were collected on a hammer or scoop, and were immediately quenched in water to stop growth of gas bubbles and devitrification. Spatter samples were watched in flight, picked up upon landing, and water quenched. Samples labeled "core" (fig. 57.21, 57.22) were from interiors of aa flows. Some were collected from thermocouple tips or hammers and quenched, but a few were collected after they had cooled naturally.

To obtain densities, the samples were diced to cubic or near-cubic form, measured, dried at 20 °C, and weighed.

APPENDIX 57.2
OBSERVATION METHODS AT CHANNEL STATIONS

Many interpretations in this paper, especially those related to lava volumes, are based on quantitative measurements at the channel stations (table 57.2, fig. 57.1*B*). These measurements, though relatively straightforward, involve some assumptions and complications that require further explanation.

The initial purpose of the stations was to permit replicate measurement of channel velocities and volumes along lower reaches of the flow to document any changes in rates at which lava was moving toward Hilo. It was thought that more meaningful results could be obtained downchannel than close to the vent, where channel velocities were high and channel volumes were more influenced by short-term fluctuations in vent activity. Observations on lava flow and channel morphology were a supplemental benefit.

Sites for channel stations were chosen along relatively straight channel reaches of uniform gradient, in order to minimize perturbating effects of local channel geometry. At each station, one or more distances for timing velocities, typically 15–30 m in length, was measured and flagged close to the channel bank, along with sighting points located farther back and perpendicular to the channel. Most lava-velocity measurements were thus made by two observers at these sighting points, timing the motion of identifiable channel material along the measured course. Multiple measurements were made, typically 5–10, until consistent results were obtained. Anomalously slow values, mostly related to material that deviated from center channel, were discarded. The others were averaged; the range of values was typically less than 10 percent. At lower channel stations affected by lava surges, some measurements were made during surges, but plotted values (fig. 57.26) were determined during seemingly representative intervening periods. Helicopter-transport logistics commonly permitted or required several hours of observation at each station.

Most such measurements were made on lava boats and large readily identifiable blocks of floating debris near center channel, but at some stations (especially along upper channel reaches where velocities were high), the lava boats traveled more slowly than small pasty debris on the lava surface. In addition, the lava boats tended to migrate from the highest velocity zone in center channel into slower moving marginal zones (fig. 57.10). At such stations (for example, 1852 vent), a single observer had to make the entire measurement from one sighting point, in order to follow difficult-to-identify channel fragments. Accordingly, a diagonal sighting point was established, aimed at center channel on line with the lower observer point. This procedure empirically yielded consistent results, even though inherently more prone to measurement error because of unfavorable geometry for comparing velocities of lava fragments that deviated slightly from center channel.

Within a kilometer of the vent, the cross-flow velocity gradient again became abrupt at the channel edges (fig. 57.10, station 11), but there were relatively few lava boats for timing velocities. In these areas, the channel lava was essentially foam, and we measured velocities by throwing in a piece of levee lava (which sank) and timing the velocity of the resulting dimple in the lava surface.

While surface channel velocities were thus measurable with considerable precision, translation of such values into lava volumes required determination of cross-sectional channel geometry values which involve greater uncertainties. Channel breadth was measured directly at the station by use of an optical rangefinder, if heat shimmer did not interfere, or was estimated from a hovering helicopter by reference to the surveyed distances along the channel bank. Channel depth could be estimated by (1) constraints of pre-eruption topography, (2) limits indicated by the size of the largest lava boats, and (3) profiles of drained channels after cessation of the eruption (fig. 57.18). Factor (1) provided broad constraints, especially for upper channel stations where total flow thickness appeared to be only about 4–6 m, but local irregularity in surface topography precluded detailed estimates based on overall flow thickness. Observation that some large lava boats grounded and rolled (2), especially at low channel levels between surges, provided key channel depth data for some stations. Examination of drained channels after the end of the eruption (3) provided minimum depth estimates for some stations; interpretation of such values was complicated by incomplete draining, by burial of some stations during stagnation of the flow system, and by changes in channel geometry during the eruption. Possible sedimentation and erosion of the channel floor are recognized problems of lava flow evolution, to which we can add little. Channel overflows and levee growth more than doubled the flow thickness at several stations during the eruption.

Beyond such measurements and estimates of the channel cross-sectional geometry, additional uncertainties involve variations in velocity laterally and vertically in the channel, as well as protrusion of the lava lens beneath the channel banks in the transition zone (fig. 57.5). Lateral velocity gradients on the channel surface, noted above, were especially prevalent in the stable channel zone, where fivefold velocity gradients from center channel to margins were common. Intricate eddies and even reverse flow, analogous to any high-energy water stream, were also common. Surface gradients were more modest downchannel (transition zone), where plug flow commonly characterized most of the active channel and only a narrow marginal zone a few meters wide was characterized by a strong velocity gradient. In addition, poorly understood vertical velocity gradients, with velocity decreasing downward in the channel, are demonstrated by the commonly slower velocities measured for lava boats with sizable keels, in comparison with smaller surface debris on the channel surface. Finally, the process of kneading out gas bubbles, as lava flowed downchannel, may well have been increasingly effective with depth in the channel, producing a vertical density zonation in the lava channel. All these complications contribute to uncertainties in the lava-volume measurements that are difficult to resolve quantitatively.